CFD Analysis of Wind Concentrator

[1]Md Ahsan, [2]Ramniwas Bishnoi, [3]Sanjeev Kr. Singh

Department of Mechanical Engineering, Niet- Nims Institute of Engineering & Technology
NIMS University, Jaipur, India

Abstract: **Wind energy provides an attractive power source as an alternative to fossil fuels because it is abundant, clean, and produces no harmful emissions. To extract more energy from the wind we need to increase the wind turbine size. However, the increase in size has begun to reach a limit in terms of material composition and structural stability. To quell the trend of increasing size in wind power systems alternative wind turbine blade designs are investigated and evaluated to increase power production and efficiency of present size machines. Wind concentrators have been proposed for the turbulence flow and low velocity region because they provide structural and aerodynamic advantages.**

In this study, several selected concentrator designs were analyzed. A computational fluid dynamics (CFD) program was used to model air flow patterns through a prototype wind concentrator and optimize its performance. Through this method, it was determined that a concentrator with a disk shaped entrance and exit is effective at concentrating wind energy.

Maximum velocities were obtained with the addition of pressure-relief slits in the inlet v portion. With an ambient inlet air stream of 8 m/s, CFD results predicted the concentrator would accelerate the air velocity to 18.56 m/s. The concentrator also predicted similar accelerations at higher inlet velocity. Our numerical simulations show that the circular disk shaped wind concentrator can increase velocity approx twice the inlet.

I.   INTRODUCTION

1.1 Wind Energy

Wind energy is the kinetic energy of air in motion, also called wind. Total wind energy flowing through an imaginary area A during the time t is:

$$E = \frac{1}{2}mv^2 = \frac{1}{2}(Avt\rho)v^2 = \frac{1}{2}At\rho v^3,$$

where ρ is the density of air; v is the wind speed; Avt is the volume of air passing through A (which is considered perpendicular to the direction of the wind); $Avt\rho$ is therefore the mass m passing per unit time. Note that $\frac{1}{2}\rho v^2$ is the kinetic energy of the moving air per unit volume.

Power is energy per unit time, so the wind power incident on A (e.g. equal to the rotor area of a wind turbine) is:

$$P = \frac{E}{t} = \frac{1}{2}A\rho v^3.$$

Wind power in an open air stream is thus *proportional* to the *third power* of the wind speed; the available power increases eightfold when the wind speed doubles. Wind turbines for grid electricity therefore need to be especially efficient at greater wind speeds.

Wind is the movement of air across the surface of the Earth, affected by areas of high pressure and of low pressure. The surface of the Earth is heated unevenly by the Sun, depending on factors such as the angle of incidence of the sun's rays at the surface (which differs with latitude and time of day) and whether the land is open or covered with vegetation. Also, large bodies of water, such as the oceans, heat up and cool down slower than the land. The heat energy absorbed at the

Earth's surface is transferred to the air directly above it and, as warmer air is less dense than cooler air, it rises above the cool air to form areas of high pressure and thus pressure differentials. The rotation of the Earth drags the atmosphere around with it causing turbulence. These effects combine to cause a constantly varying pattern of winds across the surface of the Earth.

The total amount of economically extractable power available from the wind is considerably more than present human power use from all sources. Axel Kleidon of the Max Planck Institute in Germany, carried out a "top down" calculation on how much wind energy there is, starting with the incoming solar radiation that drives the winds by creating temperature differences in the atmosphere. He concluded that somewhere between 18 TW and 68 TW could be extracted. Cristina Archer and Mark Z.Jacobson presented a "bottom-up" estimate, which unlike Kleidon's are based on actual measurements of wind speeds, and found that there is 1700 TW of wind power at an altitude of 100 metres over land and sea. Of this, "between 72 and 170 TW could be extracted in a practical and cost-competitive manner". They later estimated 80 TW. However research at Harvard University estimates 1 Watt/m^2 on average and 2–10 MW/km^2 capacity for large scale wind farms, suggesting that these estimates of total global wind resources are too high by a factor of about.
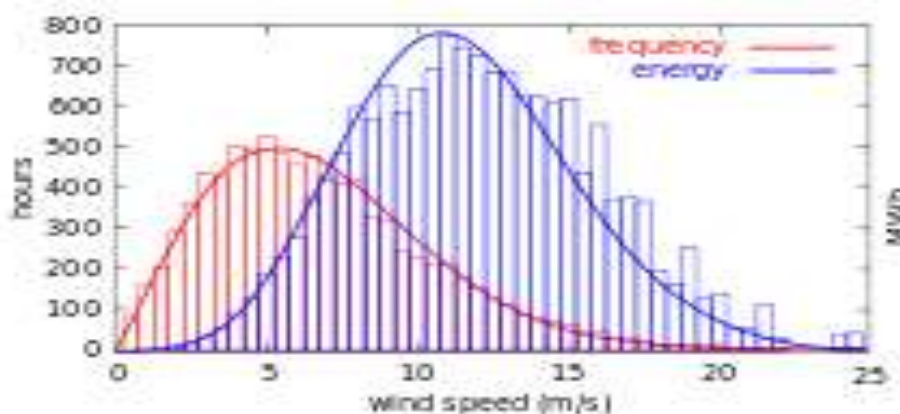
1.1.1 Distribution of wind speed

Fig.1: (Distribution of wind speed (red) and energy (blue). The histogram shows measured data, while the curve is the Rayleigh model distribution for the same average wind speed.)

The strength of wind varies, and an average value for a given location does not alone indicate the amount of energy a wind turbine could produce there. To assess the frequency of wind speeds at a particular location, a probability distribution function is often fit to the observed data. Different locations will have different wind speed distributions. The Weibull model closely mirrors the actual distribution of hourly/minute wind speeds at many locations. The Weibull factor is often close to 2 and therefore a Rayleigh distribution can be used as a less accurate, but simpler model.

1.1.2 High altitude winds

Power generation from winds usually comes from winds very close to the surface of the earth. Winds at higher altitudes are stronger and more consistent, and may have a global capacity of 380 TW. Recent years have seen significant advances in technologies meant to generate electricity from high altitude winds.

1.2 Wind Concentrator

1.2.1 History

It was recognized by Betz, as early as 1926 , that there was a theoretical upper limit to the amount of energy that can be extracted from the wind energy flux which is available to a wind turbine of given dimensions. His simple theory was amended by taking into account the influence of rotation left behind in the wake of the wind turbine, but this reduced the attainable amount of wind energy even further, not to mention the inevitable friction losses (profile drag). Also due to the low energy density of the wind, wind turbines of very large diameters have to be applied to produce a significant amount of energy. In order to get around this limitation, a number of devices have been proposed, with the purpose to concentrate

the wind stream to a smaller area (increased mass flow). The increased energy output for a given diameter has then to be weighed against the cost increase due to the added structural elements. The purpose of this Chapter is to discuss the various concepts of increasing the power output. Therefore, the cost-effectiveness of a wind concentrator will not be discussed, but the possible adverse effect of the additional costs on the feasibility of a wind concentrator concept has to be kept firmly in mind.

Because of the vital place of the Betz limit in this discussion, his formula will be deduced in full detail. It must be noticed that the Betz limit applies to horizontal-axis as well as to vertical-axis wind turbines. Most of the wind concentrator concepts are, however, proposed for horizontal-axis turbines. From the discussion of the Betz limit it follows that the power output of a wind turbine with a given diameter may exceed this limit, when it would be possible to increase the mass flow through the turbine. An increased mass flow can only be realized by a further reduction of the pressure in front of the turbine and a consequently increased pressure recovery towards the free-stream pressure behind the turbine. By a number of investigators it was found that the application of a diffuser behind the wind turbine should have the desired result. The original ideas were concentrated on the conventional diffuser, but it was realized that, in order to limit the size of such a device, an annular wing or "shroud" could operate more efficiently, especially as regards the costs of the structure. In this respect it has to be noticed that a diffuser-type augmentor has to be put into the wind direction, though a "bell-mouth" intake in front of the turbine alleviates this restriction substantially. The diffuser augmentor could be used in combination with a vertical-axis turbine, but, in that case, the wind-direction independence of the vertical-axis turbine is lost and the additional advantages of a shrouded horizontal-axis turbine, such as a reduction of tip losses, cannot be obtained.[1]

1.2.2 Momentum and Energy Equation:

Theoretically when the flow is gradually varied, energy and momentum equation should yield same results. Consider a gradually varied flow. The pressure distribution in the sections is taken as hydrostatic, the channel bed slope as small. For a rectangular channel of small slope and width b, in a short reach the expression for pressure forces This equation appears to be practically the same as the energy equation (Bernoulli equation). However, the energy loss given by momentum equation is due to external forces whereas the loss given by energy equation is due to internal forces. One is a vector quantity and other is scalar quantity. The difference between α and ρ is ignored. Similarity ends here. There are cases where **either momentum equation or energy equation can be used with the continuity equation.**[4]
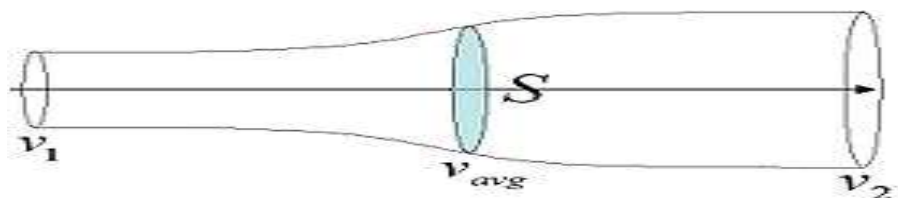
1.2.2.1 Betz' law:-

Fig: 2 Schematic of fluid flow through a disk-shaped actuator. For a constant density fluid   cross sectional area varies inversely with speed.
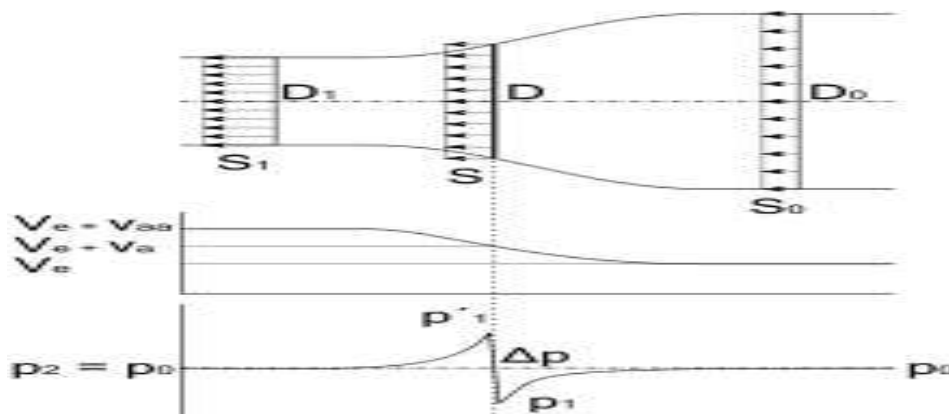

Fig.3: An actuator disk accelerating a fluid flow from right to left.

In fluid dynamics, the **momentum theory** or **disk actuator theory** is a theory describing a mathematical model of an ideal actuator disk, such as a propeller or helicopter rotor,

The rotor is modeled as an infinitely thin disc, inducing a constant velocity along the axis of rotation. The basic state of a helicopter is hovering. This disc creates a flow around the rotor. Under certain mathematical premises of the fluid, there can be extracted a mathematical connection between power, radius of the rotor, torque and induced velocity. Friction is not included.

For a stationary rotor, such as a helicopter in hover, the power required to produce a given thrust is:

$$P = \sqrt{\frac{T^3}{2\rho A}}$$

Where:

- T is the thrust
- ρ is the density of air (or other medium)
- A is the area of the rotor disc

Betz's law calculates the maximum power that can be extracted from the wind, independent of the design of a wind turbine in open flow. The law is derived from the principles of conservation of mass and momentum of the air stream flowing through an idealized "actuator disk" that extracts energy from the wind stream. According to Betz's law, no turbine can capture more than 16/27 (59.3 percent) of the kinetic energy in wind. The factor 16/27 (0.593) is known as Betz's coefficient. Practical utility-scale wind turbines achieve at peak 75% to 80% of the Betz limit.

The Betz limit is based on an open disk actuator; if a diffuser is used to collect additional wind flow and direct it through the turbine, more energy can be extracted. However, such shrouded turbines are costly to build in utility-scale units because of the extra structure required.
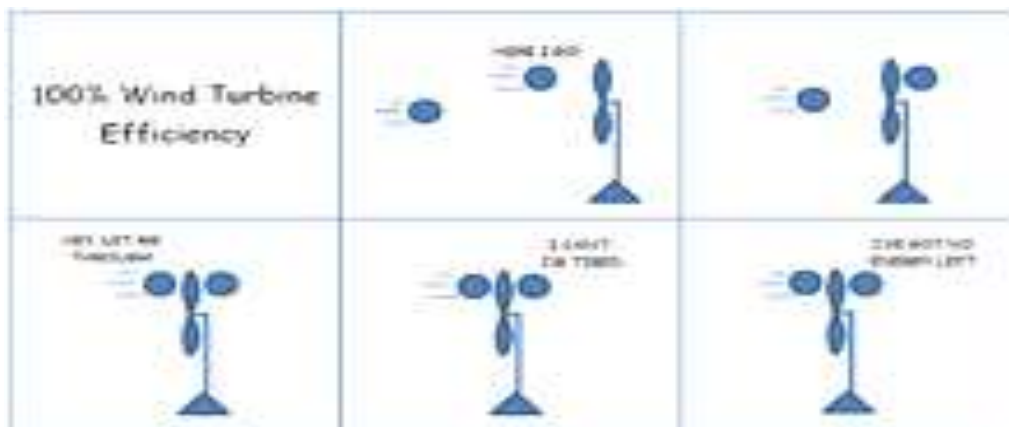
1.2.3 Concepts of Wind Turbine

Fig:-4. Simple cartoon of two air molecules shows why wind turbines cannot actually run at 100% efficiency.

Consider that if all of the energy coming from wind movement into the turbine were extracted as useful energy then the wind speed afterwards would drop to zero. If the wind stopped moving at the exit of the turbine, then no more fresh wind could get in and it would be blocked.

In order to keep the winds moving through the turbine there has to be some wind movement, however small, on the other side with a wind speed greater than zero. Betz' law shows that as air flows through area, and when it slows from losing energy to extraction from a turbine, it must spread out to a wider area. Geometry is what limits the turbine efficiency to 59.3%.[7]

Def. – *Wind Concentrator* is defined as a casing in which the wind is collected and concentrated to be forcibly guided against the blades of a rotor.

1.3 Types of Wind Concentrator:

I. The first type consists of a *obstruction type* which increases the wind kinetic energy available for harnessing. In this a vertical cylinder or vertical flat surface is used to produce high local velocities around two counter-rotating vertical axis rotors.

II. The second type is *a cylindrical Darrieus rotor*, which acts like a porous cylindrical obstruction to the wind. For high solidity rotors the inner blockage will increase the wind speed experienced by those blades that operate near the maximum width.

III. The third type is the *wing tip vortex* type concentrator, based on creating a horizontal tornado-like vortex with its axis aligned with the wind. A horizontal vortex is generated by a vertical high lift wing of finite span. The high local wind kinetic energy inside the vortex is harnessed by a horizontal axis rotor.[1]
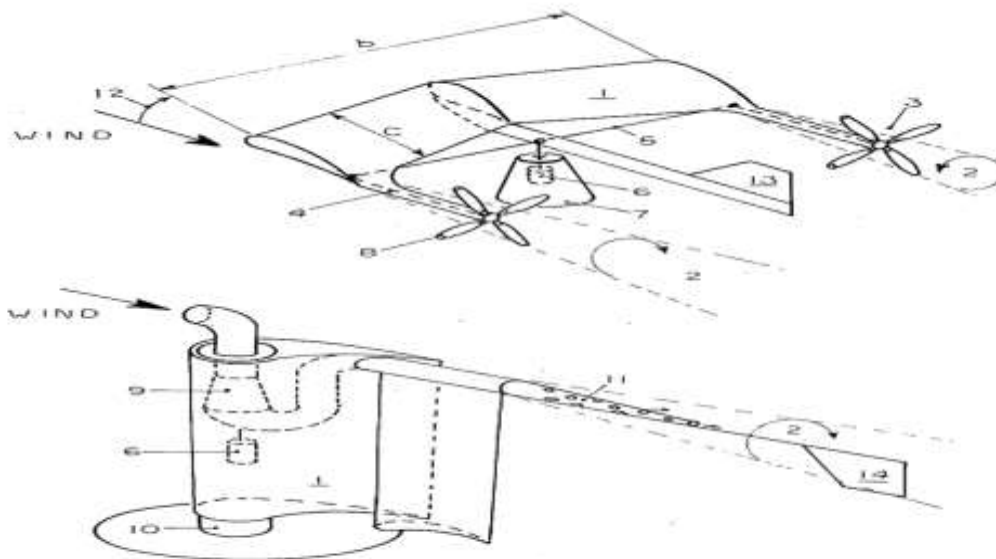

Fig 5:- Horizontal wind energy concentrator   **Fig 6:- Vertical wind energy concentrator**
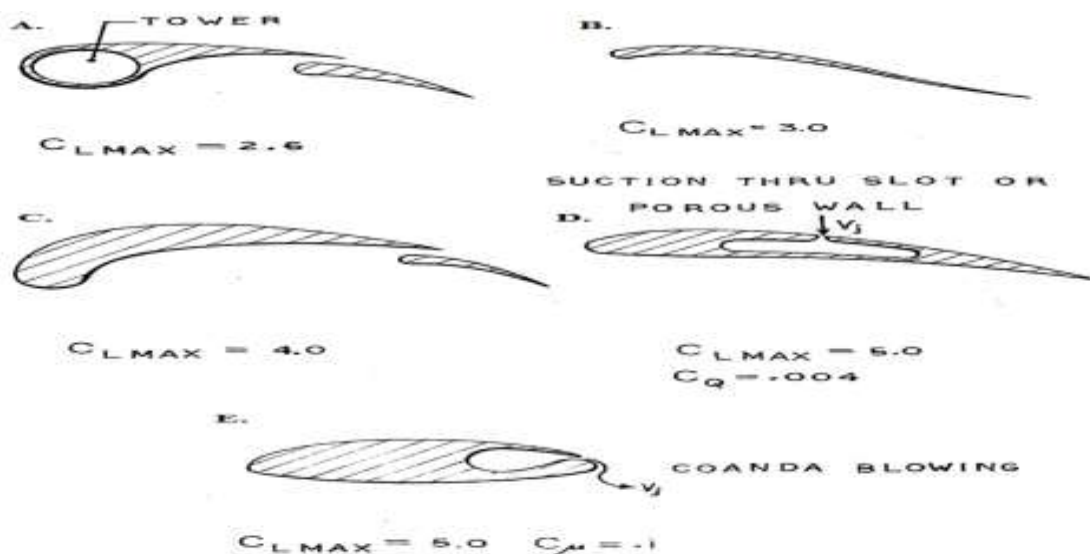

Fig 7:- Configuration of wind concentrator

Brief Description of Fig. 4

The novel feature of the invention are set out with particularity in the appended claims , but the invention will be understood more fully and clearly from the following detailed description of preferred embodiments of the invention as set forth in the accompanying drawings, in which:

A. Cross section view of a first airfoil for use in the wind energy concentrators of the present invention;

B. Cross section view of a a second airfoil for use with the wind energy concentrators of the present invention;

C. Perspective view of a third airfoil for use with the wind energy concentrators of the present invention;

D. Cross section view of a forth airfoil for use with the wind energy concentrates of the present invention; and

E. Cross section view of a fifth airfoil adapted for use wind energy concentrators of the present invention.

1.4 Wind Concentration and Low Velocity Turbines

Wind turbines are the product of convergent technological evolution in most agrarian societies. The technology that later developed into the first windmill arose out the need to grind large amounts of grain. An efficient method of grain grinding is a necessity in any society with such a staple food source. As a society grows so too does its need for food and therefore the need for manual labor.

Historians assert that it was the Egyptians who created the first windmills in 3,000 BC. Regardless of its first inventor, the technology sprung up in most agrarian societies within the next millennium. Farmers of this era devised two families of techniques to boost their ability to process grains. The first was a horizontal mill. Here, a beast of burden would pull a lever attached to a grinding wheel at the other end of the lever, marching in a circle around a central pestle, effectively grinding larger quantities of grain. These two archetypes later evolved into the two types of turbines seen today – the vertically rotating turbine and the horizontally rotating turbine – replacing either animal or water power with wings to capture the power of air (Hau, 2006).

From the two families of windmills, two families of energy collection technologies have arisen. The first is the collection of vertical axis rotors. These consist of three primary rotor designs: the Savonius Rotor, the Darrieus Rotor and the H-Rotor (See Figure 8). The Savonius is S-shaped when viewed from above. This shape allows it to act like a stretched cup-anemometer. A single sheet of metal is bent to form the S-shape. Each curve of the S acts as a cup, catching a breeze and turning the axel. This design has no direction-of-interest, unlike horizontal axis rotors, and will catch wind coming from any direction.

The Darrieus rotor is less bulky than its Savonius cousin. In this design, the blade of the rotor is shaped like a Mobius strip held vertically, creating a contoured loop. While it does not "cup" the wind like a Savonius, the curvature of the strip causes one side to present less resistance during a gust of wind, forcing the blade, and therefore the axel to spin. This design uses comparatively little resources, but captures less energy.
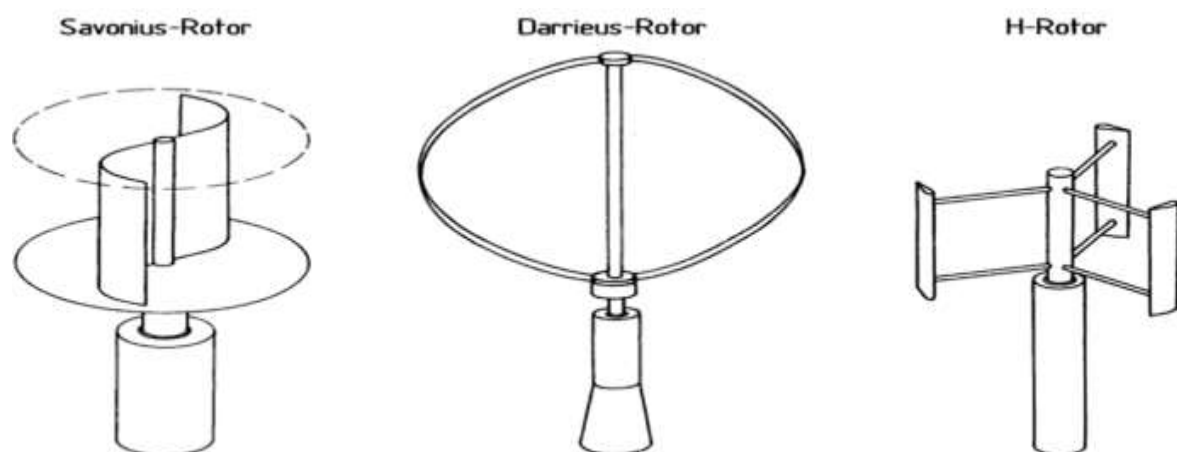

Fig. 8. Various Vertical Axis Wind Turbine Designs (Hau, 2009)

A vertical axis rotor has little means of wind concentration. The necessity of radial symmetry keeps modification to a minimum. Forgoing one direction in favor of wind concentration removes this important benefit. A rotor has a certain threshold speed before it will become useful. With vertical axis generators, it is usually only nature who may engineer this. Wind concentration is a taboo area for vertical axis generators. However, they may be adapted for low velocity conditions by attempting to lower their threshold speed to allow their use.

Some radially symmetric structures may act as wind concentrators for vertical axis rotors. Occasionally, when other solar energy capture operations are unavailable, a large metal sheet will act as an energy capture mechanism for a wind generation project. This sheet would have a tube rising from the center and be elevated a few inches above the ground. As solar radiation heats the sheet, the air beneath it heats, becoming less dense and moving through the tube in the center of the assembly. This area of rapid air flow can be fitted with a vertical generator or a more conventional turbine. Still, designs of this nature are better classified as solar power than concentrated wind power.

For a vertical axis rotor, one of the best understood means of concentration is to nest one rotor within another. This is shown above in Figure 8, as two of the low velocity designs use a Darrieus rotor to act as a vortex generator of Savonius rotors inside. When even this is not enough, engineers may design a super-structure around the inner dynamo. Victor Walters created one such schematic, patented as "Walter's Whirl-Wind."

It consists of two similar concentric assemblies of airfoils. The first is the outer right, with a diameter nearly triple the inside ring. This ring's purpose is to capture and propel air into the second ring, which used a dynamo to capture the momentum of the masses of air flowing into it. Despite being over fifteen years old, his patent and idea has done little within the industry. Concentric designs may provide a starting point for optimization, but do little for lowering the threshold of usefulness for a vertical axis rotor (Edwards, 1996).

For horizontal axis rotors, there is far more that may be done to improve the effectiveness of a land investment to wind energy. Engineers may use larger structures like ducts and cones without the symmetrical concerns related to vertical rotors. These structures either increase the effective area covered by the rotors or increase the incoming wind velocities.

Wind concentrators take four major forms. The first is a shroud for the rotor, much like the sheath over the tail rotors of helicopters, preventing incoming air from being batted away by the spinning rotors and allowing more of the momentum to be transferred. The second is a funnel at the outgoing end of the turbine, often used in conjunction with a shroud. This design, called a diffuser, appears counter-productive, as the entire device looks backwards (See Figure 3). However, through research, it has been shown that a solid funnel in front of a rotor will actually hinder air from through the device (which is why a working forward funnel design is so unique). Instead, a diffuser behind the rotor pulls air through the center of the device as it a current of air must either move through the rotor, or expend even more energy to accelerate and compress down the length of the device before rejoining the bulk air body beyond the funnel.
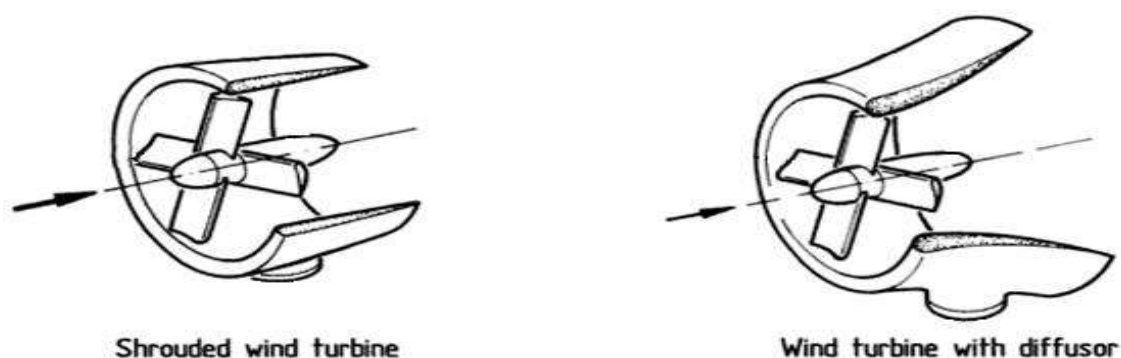

Fig. 9. Turbine with Shroud or Diffuser (Hau, 2006)

In addition to a diffuser, an airfoil may be used behind the rotors to created increased airflow due to the principles of lift. The devices, called delta wings for their triangular profiles, extend behind a rotor. These devices are often coupled, forming a bilaterally symmetrical two-rotor generator. Their usage is limited however, as their predicted benefits do not exceed their prohibitive costs and large space requirements. The last family of designs contains futuristic looking rotors that use one stationary array in front of the actual power rotor. The stator here is much larger than the rotor, and contains a structure to "herd" more air molecules into the rotor. The prohibitive cost and mechanical difficulties associated with

these has been a limiting factor in their deployment. However, for smaller generators, many mechanical problems become less important due to the reduced mass – these high tech turbines are becoming a focus for energy independence advocates (Hau, 2006).

An example of a simple shroud would be a roof-top wind generator, much like the type Glen Kane investigated in a recent patent. A shrouded turbine is aesthetically pleasing, blending into whatever it is embedded into, and requires a small land investment compared to other designs. In Glen's schematic, the turbine would be part of an assembly that could be built as a unit and installed on the peaks of roofs, mimicking the appearance of a dryer exhaust or air-conditioning intake. The small size of the invention limits its usefulness, and the shroud does little work concentrating wind sources, further bounding this device to only be used in high-wind areas. Shrouds are rarely seen alone on generators – for the price of a shroud, a diffuser could be installed, slightly increasing the required land investment and decreasing the aesthetics, but nearly doubling the wind velocity coming through the rotor aperture (Kane, 2010).

This is shown by the commercial success of the Wind Tamer turbine as a personal power source. This Wind Tamer is a shrouded rotor with a diffuser at the wayward end. While it is aesthetically designed for marketability, it contains the important elements of a diffuser. The product appeals to those in moderate wind areas. Even in favorable locations, most turbines require a high relative elevation to run efficiently, often over a hundred feet. Through the use of a diffuser, the Wind Tamer will generate energy at just twenty feet, complying with most city-zoning laws. Diffusers have shown the most commercial success for small rotor designs, and have formed a lucrative sub-market within the wind power industry. The design is built from plastics with a high strength and low cost. Additionally, due to the relatively slow wind speeds the Wind Tamer will experience, the device can afford to be more "frilly" and complex with the concern of excessive sheer stress (Wind Tamer "Comparing Wind Technologies," 2010).
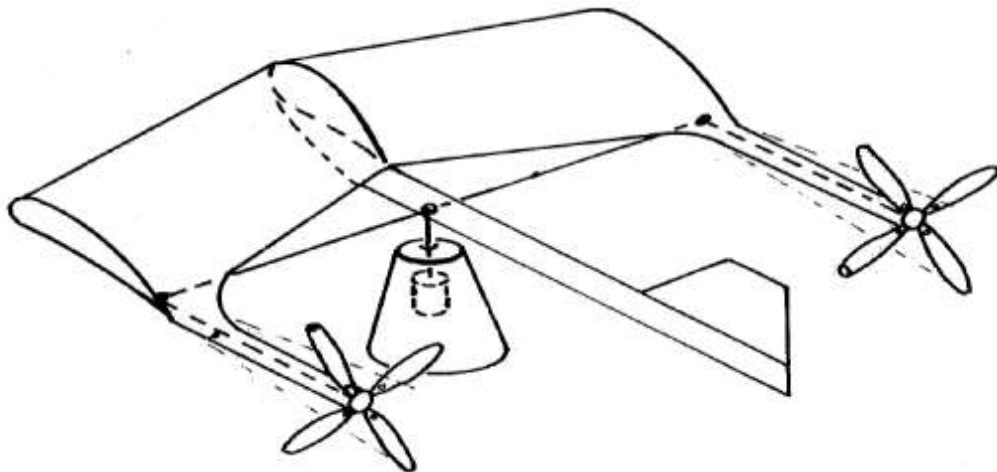

Fig.10. Loth's Turbine (Loth, 1977)

He submitted a patent in the mid-70s for a delta wing design (See Figure 10). It featured two rotors training behind a single solid wing, resembling a horizontally-laid staple, with a rotor at each end and an airfoil forming the center bar. This patent has even had time to become public domain, and still nothing has come of it (Loth, 1977).

The last family of rotors is also the most varied and has no distinct representative as with many of the categories above. The front-mounted diffuser mentioned above would actually fit more easily into this category, though it would be similarly ill-fated (Hau 2006).

1.5 Computational Fluid Dynamic

Computational Fluid Dynamics (CFD) is the analysis of systems involving fluid flow, heat transfer, and chemical reactions, by means of computer based simulation. In CFD analysis begin with a mathematical model of a physical problem and during the process conservation of matter, momentum, and energy must be satisfied throughout the region of interest .It is a tool that complements theory and experiments [6]. It is both a research tool and design tool. In this simulation fluid properties are modeled empirically and simplifying assumptions are made in order to make the problem tractable (e.g. steady state, incompressible, two dimensional).
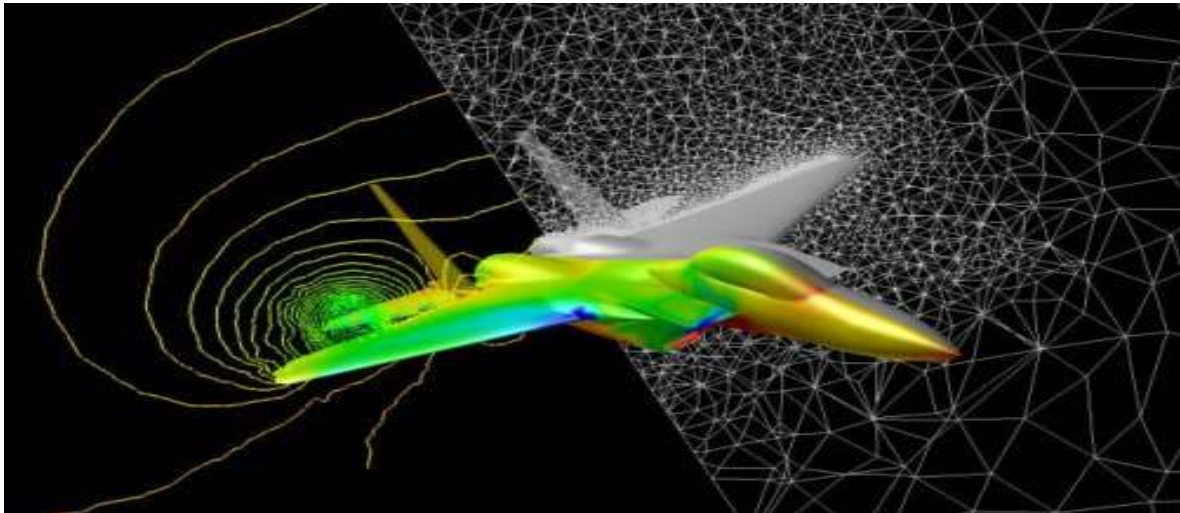
Fig.11. CFD Analysis

It has lagged behind Developments in stress analysis codes. The main advantages of CFD over experiments are reduction in lead time and cost of new designs, ability to study systems where controlled experiments are difficult to perform .Now a Days CFD has wide range of applications in various streams but some of the major areas in which CFD plays a dominating role are Aerospace Industries, Automobiles and Engine Industry, Appliances, Boats, Computers etc. Technology has provided ways to incorporate turbulent or external forces which allows engineers to create "real world" models for fluid systems. For modeling forces through a wind concentrator, one would use a equation set that incorporates friction and turbulence into the momentum balances, as well as gravity (although because a pocket of air exists in an environment of equal density, this may be safely ignored). Additionally, it must include robust equations of state that incorporate factors such as density change with temperature and pressure in its calculations.

CFD codes are structured around the numerical algorithms that can tackle fluid flow problems it has three main elements. These three main elements are (a) Pre Processor (b) Solver (c) Post Processor.

(a) Pre Processor: It consists of input of a flow problem to CFD. In this element user have to define geometry and generate grid. It takes 50% of time and than selection of phenomenon to be modeled and definition of properties and than in final selection of boundary and initial conditions take place.
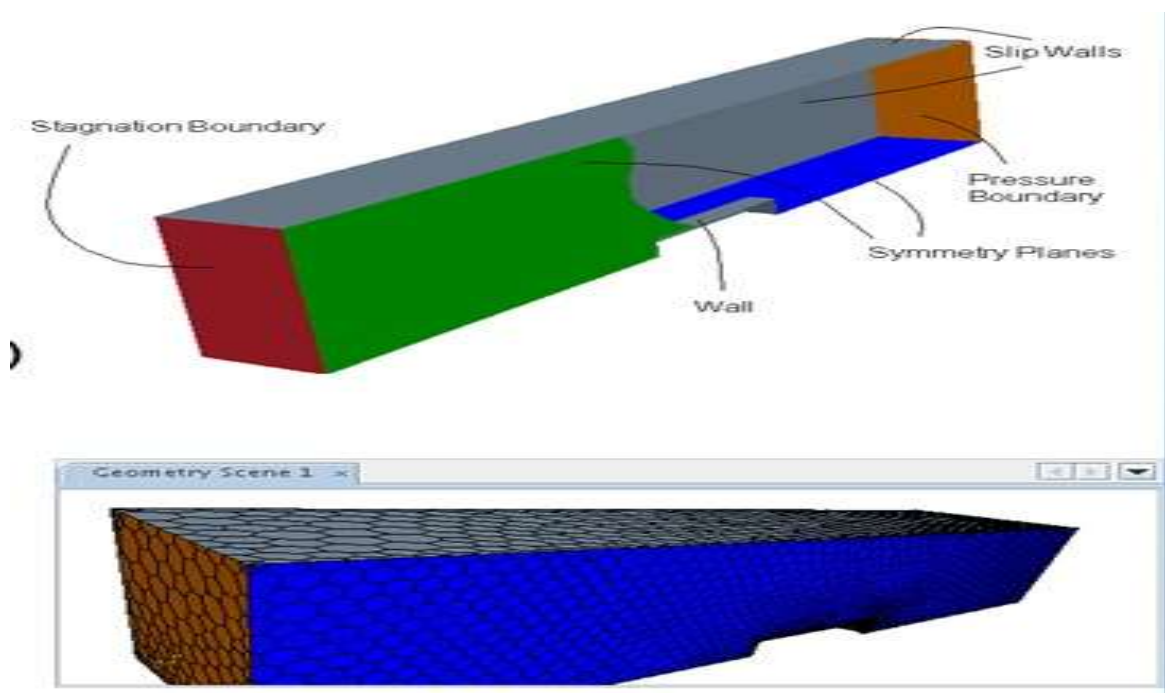

Fig. 12. Geometric model

(b) Solver: - In this element of CFD code three primary numerical solution techniques are used and these techniques are finite differences, finite element and finite control volume. The numerical method performs approximates the unknown variables by simple functions. Is performs the discretization by substitution of the approx imitations into the governing flow equations and subsequent mathematical manipulations

(c) Post Processor: - It provides a user friendly way to look at the result of simulation. in this part first of all domain geometry and grid display is in below fig
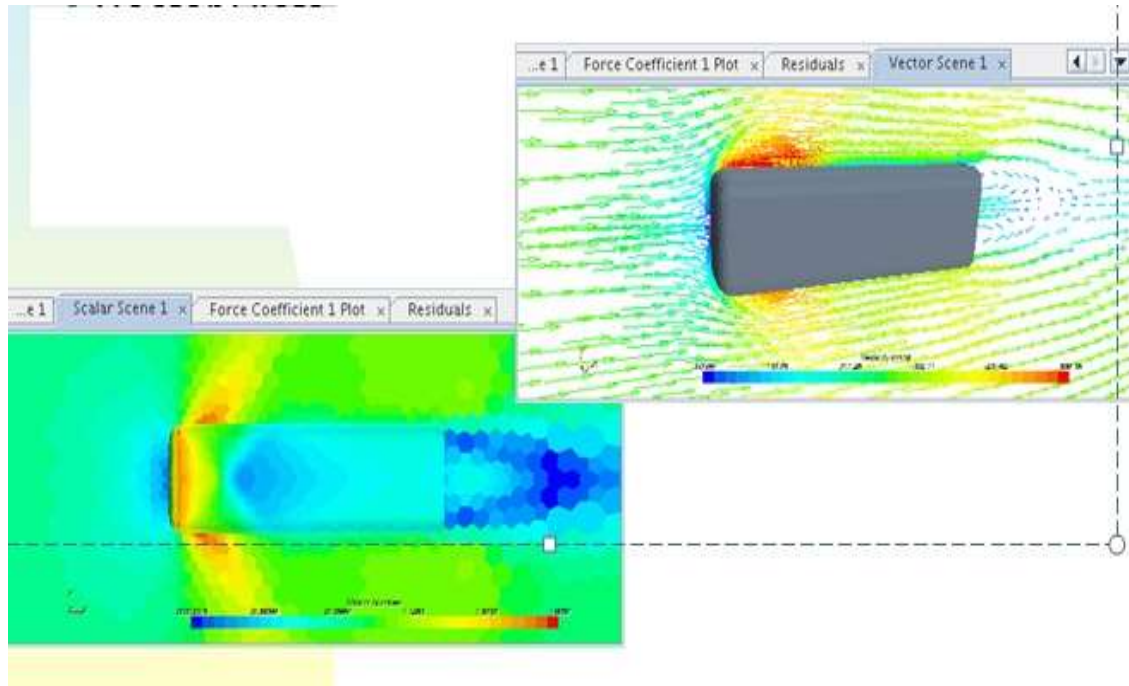

Fig. 13. Domain geometry and grid display

Shown after that vector plots, contour Plots and Particle Tracking is displayed.

Results of CFD are at best as good as the Physics embedded in it as at worst as good as its operator.

II.   LITERATURE REVIEW

2.1 Wind Speed And Energy Yield Analysis Of Small Wind Turbines On A 45m High-Rise Building In The Built Environment. [Kimberly L. King, Loughborough University Loughborough, Leics Le11 3tu]

2.1.1 Introduction

The literature review of published articles, peer-reviewed journals, reports and conference proceedings will progress in-perpetuity whilst this project is in-progress.

Aim is to perform a comparative computational fluid dynamics (CFD) data analysis of simple, average wind speeds of rooftop mounted wind turbine (WT) energy yields. Furthermore, the objective of this project is to perform a comparative investigation the performance parameters of small WT generators (<10Kw rated power), looking at simple average wind speed relationship based on the lowest part of the boundary layer (BL). And, in doing so, create a benchmark to represent an exacting, helpful standard that industry and policy makers can use by attempting to discern at what height does a small WT generator become financially feasible in the urban or built-environment.

Ultimately, to discern if there are indeed opportunities in the urban environment where a 4 m/s wind resource for an urban wind turbine could provide economic parity in cost effectiveness with photovoltaic (PVs).

 Below is a sample compendium of published articles, peer-reviewed journals, reports and conference proceedings reviewed thus far for this project. A synopsis of each follows.[2]

2.1.2 Conclusion

2.1.2.1 The Urban Wind Turbine

A. Small wind turbines for the built environment

This document explores the technical potential of small wind turbines on buildings and investigates manners in which the new wind turbine designs can meet the requirements for installation into the built environment. This document provides enlightenment on existing examples of urban wind turbines, potential markets for small wind turbines, requirements for wind turbines i0n the built environment, locating of wind turbines on buildings, novel wind turbine designs developed for building installation, and opportunities for architects to develop integrating wind turbines in building designs.

B. Wind energy in urban areas, concentrator effects for wind turbines close to buildings

This read, explores a concept that is often overlooked that energy from the wind could be produced close to where it can be used, as such, in the built environment. Technology and design issues in the use of wind energy in the built environment are discussed including suitable wind turbine designs and suitable positioning of the wind turbines.

2.1.2.2 Energy yield

A. Estimating the Potential Energy Yield of Small Domestic Roof-Mounted Wind Turbines

Employing corrected Wind Atlas data to match the built environment, this text investigates how different housing geometries and arrangements of these structures can have an effect on the local wind speed.

B. Estimating the Potential Yield of Small Buildingmounted Wind Turbines

Utilizing computational fluid dynamics (CFD) model ANSYS CFX, this paper models wind flow around a house in isolation in within an array of similarly configured houses to show the level of speed-up effect around the top and sides of a house.

C. The energy yield of roof-mounted wind turbines

A pioneering effort, the main thrust of this paper concerns developing flow features criteria to enable siting roof top wind turbines. The main building blocks covered in this paper include how one would go about ascertaining desirable height above the roof for installing a wind turbine, investigating the change of the undisturbed wind to the wind speed above the roof and the probability distribution of the wind speed above the roof. Example calculations are provided to assist the reader.

2.1.2.3 Urban buildings and infrastructure considerations

A. Sitting Micro-turbines on House Roofs

This report describes a program of wind tunnel testing that measure wind speeds above house roofs, and provides data that concerns sitting of micro-wind turbines on house roofs. It also addresses the calculation of these micro-wind turbines' power output.

B. Wind Energy in the Built Environment

Sander Mertens, pre-eminent wind energy researcher in Europe, provides information of vital interest for engineers, scientists and architects in this text. Ideas for how to maximize harvesting wind energy by utilizing building augmented wind turbines (BAWTs) address a number of mathematical models for basic concentrator configurations seen the built environment including wind turbines close to buildings, wind turbines between airfoil-shaped buildings and wind turbines in ducts through buildings. Of particular note, performance close to a building, at the roof, and at the sides of a building are offered a great deal of scrutiny.

2.1.2.4 Analysis tools and measurement techniques

A. Wind Energy in the Built Environment

Sander Mertens, pre-eminent wind energy researcher in Europe, provides information of vital interest for engineers, scientists and architects in this text. Ideas for how to maximize harvesting wind energy by utilizing building augmented wind turbines (BAWTs) whilst also considering an architectural aesthetic are addressed. This text covers basic theory of wind energy, wind characterizations and analysis tools as applied wind in the built environment, incorporating physical

and mathematical descriptions throughout. It also provides savvy, scientific analysis of three scenarios including wind turbines close to buildings, wind turbines between airfoil-shaped buildings and wind turbines in ducts through buildings.

B. Internal boundary layer growth following a step change in surface roughness

Using dimensional analysis, D. H. Wood performs tests for the simple correlation for the height of the internal boundary layer, and how it is controlled by the larger of the upstream and downstream roughness length scales.

C. Procedures for Substituting Values for Missing NWS Meteorological Data for Use in Regulatory Air Quality Models

This read discourages using data for modeling if more than 10% of the on-site surface data is missing. Applicable to this research, surface data includes wind direction and wind speed. This read provides two procedures for providing substitute values for missing data an objective procedure and a subjective procedure. The former involves applies to single isolated hours with missing surface data and single isolated days of missing mixing height data. The latter applies to longer sequences of missing data, requiring rendering of judgment calls by seasoned experimenters and modelers.

2.2 Vertical Variation Of Frequency Distributions Of Wind Speed In And Above The Surface Layer Observed By Sodar [Stefan Emeis, Institute For Atmospheric Environmental Research, Germany]

2.2.1 Introduction

10 min-averaged wind speed data have been measured with a mini-sodar for 13 months subsequently at different sites in level terrain and on hill tops in Germany in the last three years. The data presented here is from a height range between 25 and 140 m above ground, the vertical resolution is 5 to 10 m. From the data monthly mean diurnal courses of wind speed and of directional shear have been computed as well as monthly mean vertical pro. les of the scale factor and the shape parameter of the WEIBULL wind speed frequency distribution. These pro. les extend beyond the top of the surface layer into the EKMAN layer.

Therefore the pro. les have to be described by EKMAN layer laws instead of by surface layer laws if they have to be extra polated upward. Typical features of the pro. les characterizing level terrain and hill top sites have been analyzed. Most prominent feature is the maximum of the shape parameter at the top of the surface layer. Implications for the sitting of wind turbines are discussed.[2]

2.2.2 Conclusion

The mini sodar has proven to be a useful measurement device in order to measure wind pro. les in the height range between 30 and 140 m above ground. This height range extends well above the top of the surface layer for which the most common vertical extrapolation rules(e.g. the power law). Sodar measurements analyzed in this paper show the top of the surface layer between 40 m above ground over hill top sand 80 m above ground in level terrain .Thus, modern wind turbines with hub heights up to more than 100 m reach into the EKMAN-layer.

Therefore, for the estimation of the possible power output from these turbines EKMAN-layer pro. le laws like eqns. have to be used for the vertical extrapolation of the parameters of the WEIBULL wind speed and constructive comments of the two anonymous reviewers led to a considerable improvement of the paper.

2.3 Casting the Variation Of Wind Speed With Height Using Gust Factor Measurement [Dr. S. A Hsu, Professor of Meteorology at Louisian]

2.3.1 Introduction

In the atmospheric surface boundary layer from the ground level up to a few hundred feet, the wind speed normally increases with height under near-neutral conditions. Knowledge of the vertical variation of the wind speed is important to operational meteorologists so that they can provide reasonable estimates to emergency managers and structural engineers. For example, during hurricane conditions in New Orleans, Louisiana, what would be the expected wind gust on the elevated bridges crossing the Mississippi River? What would be the expected wind loading on a high-rise building which might be used as a vertical evacuation shelter? This increase in wind speed is often estimated operationally using the power-law wind profile. However, its exponent needs to be determined objectively. This note provides a solution through the utilization of gust factor measurements. It is shown that the formula $G = 1 + 2.88P$ is verified under the conditions of one tropical storm and ten hurricanes for a total of 148 samples as measured from various airports, where G is the gust factor (i.e., the ratio of wind gust to the mean wind speed) and P is the exponent of the power-law profile.[3]

2.3.2 Conclusion

Now, substituting G = 1.42 into the formulae G= 1+ 2.88P, we get P = 0.15. Since this value is the same as we conclude that can be used to get P objectively from G and then this P can confidently be employed in for operational applications such as now casting. Since it is verified, it may be applied to other environments on land if G is available. Note, that if the mean wind speed is less than 6 m S-l (or 12 kt), P is a function of not only So but also stability.

2.4 Concentrator For Built Environment

This thesis deals with wind energy conversion in the built environment. It gives a description of the wind resources in the built environment that can be converted into energy by a wind turbine. With a focus on maximum energy yield of the wind turbine, it especially deals with the integration of wind turbine and building in such a way that the building concentrates the wind energy for the wind turbine. Three different basic principles of such "buildings that concentrate the wind" or concentrators are distinguished:
1.wind turbines at the roof or sides of buildings,
2.wind turbines between two airfoil-shaped buildings,
3.wind turbines in ducts through buildings.
The aerodynamics of those three concentrators with their possible wind turbines are investigated with a focus on integration resulting in maximum energy yield of the wind turbine.[6]

The complicated concentrator effects of buildings in the actual flow are simplified to their basic aerodynamic qualities in parallel flow. The properties of these simplified qualities in parallel flow are explored through the three well-known cornerstones of aerodynamic research: mathematical models, verification with measurements and numerical simulations of the flow. The mathematical models are derived with simplified mathematical flow descriptions. The measurements are carried out in the open jet wind tunnel of Delft University of Technology, section Wind Energy and the simulations are performed with a commercial Computational Fluid Dynamics (CFD) code, which solved the basic flow equations numerically. The advantages of both verification tools: measurement and CFD calculation are exploited by pre-selecting the tool with the best prospects for an accurate result in a desired situation.

This thesis gives a broad description of the most important issues concerning the energy yield of a wind turbine in the built environment. It provides descriptions of the average/ global wind speed in the built environment, the local wind speed, the wind speed near buildings and verification of the mathematical models of the three possible concentrator principles mentioned above. Furthermore, it provides information on suitable wind turbines for use in the built environment. The pros and cons of the three concentrator principles are summarized, without mathematics, in the last chapter. This last chapter shows that the "at roofs of buildings" configuration and a variation on the "in ducts through buildings" configuration are promising. Concerning the "at roofs of buildings" configuration, a sphere-like building concentrates the energy in Omni directional free stream wind the most: a factor of three to four! Such concentrators are able to overcome the problem of the low average wind speed in the built environment and enable energy yields comparable to rural areas. A variation on the "in ducts through buildings" configuration, two ducted ellipsoids in a cross with the duct at the cross centre, is able to concentrate the energy in Omni directional free stream wind with a factor of approximately one and a half. The other concentrators provide a smaller energy concentration. The "close to a building" configuration is very efficient in using the acceleration by the building and it is a relatively cheap solution compared to the other possible concentrator principles. Still, this thesis shows that the energy yield for all concentrator configurations is limited because the wind turbines can only profit from the concentrator effects when they are relatively small compared to the building. Yet, they deliver the energy, where it is needed, the built environment, and their energy yield is felt as an energy saving in the building. It is thus concluded that wind energy conversion in the built environment making use of the concentrator effects of buildings, is a promising renewable energy source.

2.5 Modern Development

In 1935 H. Glauert derived the expression for turbine efficiency, when the angular component of velocity is taken into account, by applying an energy balance across the rotor plane. Due to the Glauert model, efficiency is below the Betz limit, and asymptotically approaches this limit when the tip speed ratio goes to infinity.

In 2001, Gorban, Gorlov and Silantyev introduced an exactly solvable model (GGS), that considers non-uniform pressure distribution and curvilinear flow across the turbine plane (issues not included in the Betz approach) The GGS model predicts that peak efficiency is achieved when the flow through the turbine is approximately 61% which is very similar to the Betz result of 2/3, but the GGS predicted peak efficiency is much smaller: 30.1%.

Recently, viscous computations based on computational fluid dynamics (CFD) were applied to wind turbine modeling and demonstrated satisfactory agreement with experiment. Computed optimal efficiency is, typically, between the Betz limit and the GGS solution.[7]

III.   OBJECTIVES

The objectives of this study were to:

1. To select a wind concentrator model for analysis using analytical methods and CFD tools.

2. To perform numerical analysis using CFD tools on selected models for different flow conditions.

3. To optimize correlation of wind concentrator area and Reynolds number.

IV.   PROCEDURE

4.1 Physical Model

We consider three circular disk shaped wind concentrator of outer radius to 7m, 8m, and 9m of inner radius 2m, 4m, and 6m respectively having thickness of 1m.

SIDE VIEW.   FRONT VIEW.
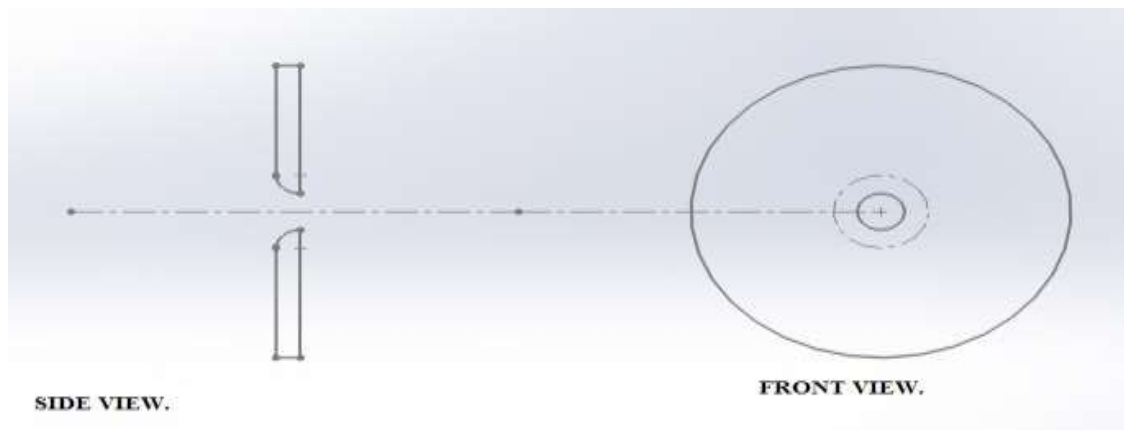
Fig. 14

The above **Fig14:** Shows, the side view and front view of concentrator having inner radius 2m

4.2 Problem Solving.

To study the effect of concentrator on Velocity, Pressure, and Reynolds's number. We determine the outlet velocity, outlet pressure and Reynolds's number on all three different model of concentrator by assuming the case that the flow is steady state, incompressible and the inlet velocity is 8m/s.

4.2.1 CASE 1: Having Dia. 2m.

Inlet   Outlet
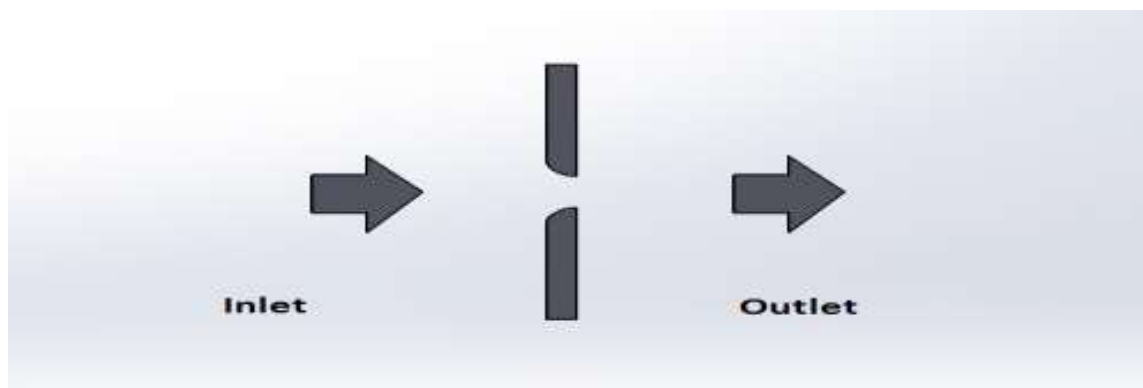
Fig. 15.

Given that;-

D= 2m. A_0= 2m.

A_1= 14m. A_2= 4m.

V_1= 8m/s, and P_1= atm. pressure.

Using Continuity Equation with coefficient of concentration.

Q= $A_1 V_1$ =$A_2 V_2$ ………………………………………………………………..(1)

V_1= $V_2 C_c$ (A_2/A_1)   Since C_c =A_0/A_2, Hence C_c= 0.5.

8=V_2* 0.5(4/14)

V_2= 56m/s.

Using Bernoulli equation:-

$(P_1-P_2)/W = (V_2^2-V_1^2)/2g$…………………………………………………………(2)

$(101325-P_2)/1*10 = (56^2-8^2)/2*10$

P_2= 99789.P_A= 0.99 atm.

R_e=$\rho v d/\mu$

R_e= (1*56*2)/1.983*10^{-5}

R_e=5.648008*10^5

Since the value of REYNOLD'S NUMBER lies between $7*10^5 \geq R_e 3*10^5$.

Hence the flow obtain will be LAMINAR.

4.2.2 CASE 2. Having Dia. 4m
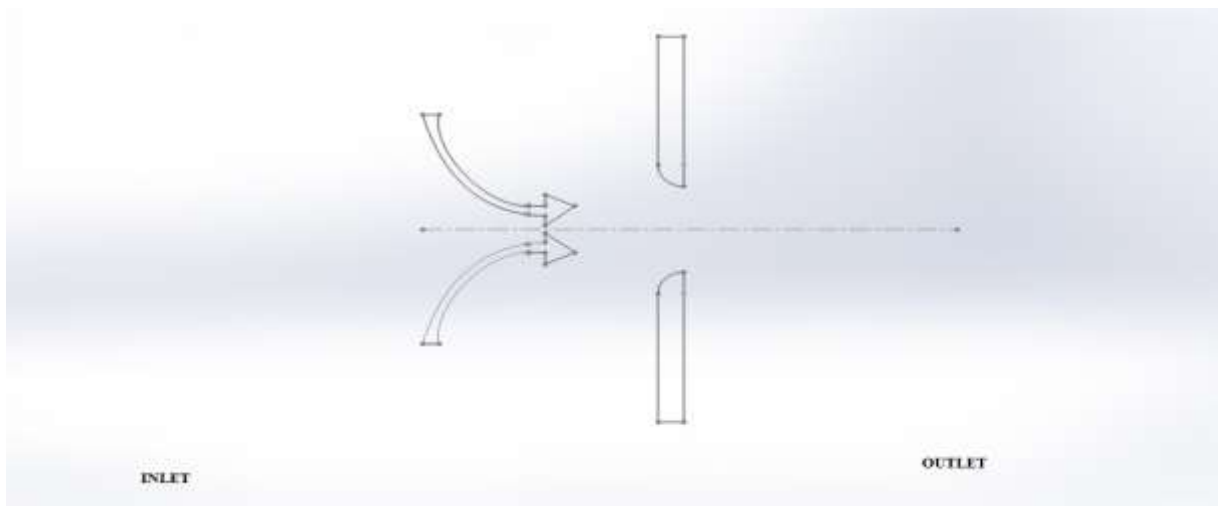
Fig. 16.

Given that;-

D= 4m. A_0= 4m.

A_1= 16m. A_2= 6m.

V_1= 8m/s, and P_1= atm. pressure.

Using Continuity Equation with coefficient of concentration.

Q= $A_1 V_1$ =$A_2 V_2$ …………………………………………………………………(1)

$V_1= V_2C_c (A_2/A_1)$ Since $Cc =A_0/A_2$, Hence $C_c= 0.66$.

$8=V_2* 0.66(6/16)$

$V_2= 32.32m/s.$

Using Bernoulli equation:-

$(P_1-P_2)/W =(V_2^2-V_1^2)/2g$……………………………………………………(2)

$(101325-P_2)/1*10 = (32.32^2-8^2)/2*10$

$P_2= 100834.7088.P_A= 1$ atm.

$R_e= \rho vd/\mu$

$R_e= (1*32.32*4)/1.983*10^{-5}$

$R_e=6.5194 10^5$

Since the value of REYNOLD'S NUMBER lies between $7*10^5 \geq R_e 3*10^5$. Hence the flow obtain will be LAMINAR.

4.2.3 CASE 3. Having Dia. 6m.
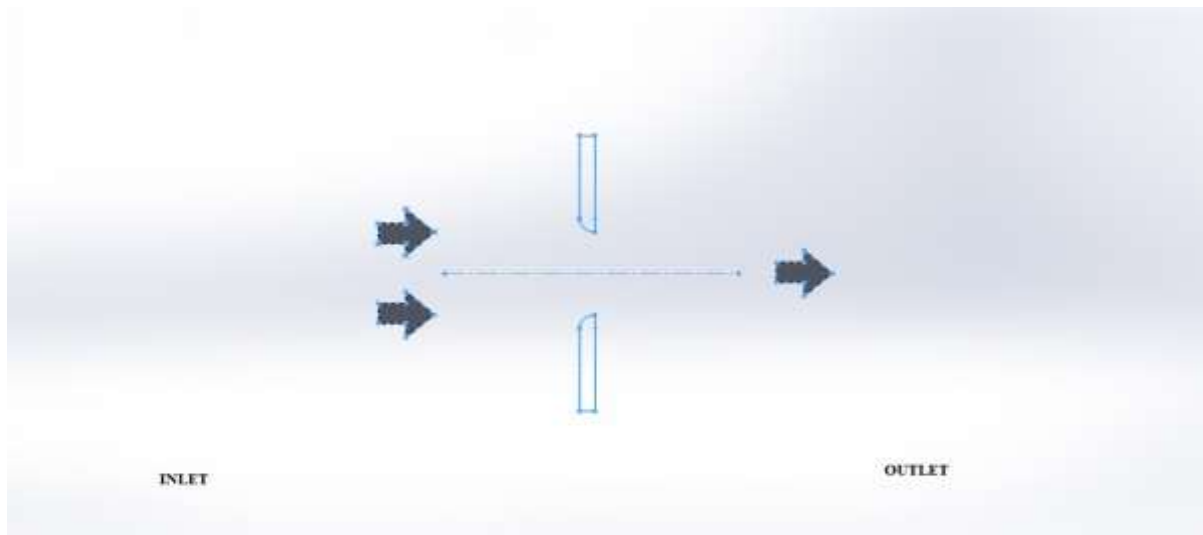
Fig. 17.

Given that:-

D= 6m. A_0= 6m.

A_1= 18m. A_2= 8m.

V_1= 8m/s, and P_1= atm. pressure.

Using Continuity Equation with coefficient of concentration.

$Q= A_1V_1 =A_2 V_2$……………………………………………………………(1)

$V_1= V_2C_c (A_2/A_1)$ Since $Cc =A_0/A_2$, Hence $C_c= 0.75$.

$8=V_2* 0.75(8/18)$

$V_2= 24.24m/s.$

Using Bernoulli equation:-

$(P_1-P_2)/W =(V_2^2-V_1^2)/2g$……………………………………………………(2)

$(101325-P_2)/1*10 = (24.24^2-8^2)/2*10$

$P_2= 101063.2112.P_A= 1$ atm.

$R_e= \rho v d/\mu$

$R_e= (1*24.24*6)/1.983*10^{-5}$

$R_e=7.334*10^5$

Since the value of REYNOLD'S NUMBER lies between $7*10^5 \geq R_e 3*10^5$.

Hence the flow obtain will be LAMINAR.

COMPUTATIONAL METHOD:

4.3 Geometry and Mesh Generation

CFD is a robust modeling program with significant synergy with the fluent modeling suite. Gambit version 2.4.6 is useful for creating the geometry of the wind concentrator system, as well as to create the complete mesh when meshing, Gambit divides these solids into a finite number of discrete elements, often consisting of tetrahedrons for 3D geometries; it can also generate hexahedral cells, or hybrids of either. Gambit can also generate a 2D surface mesh, consisting of either three or four-sided polygons. These meshes are then exported to Fluent version 6.3.26 for processing and analysis.

To model the two-dimensional flow of air through the wind concentrator, the concentrator geometry was assumed to be suspended in the center of a wind tunnel, with flow parallel to the ground. The diameter of the flow field is such that no boundary effects from its walls will affect the concentrator's efficiency. The concentrator array is located in the center of this cylinder shaped wind tunnel. The easiest way to construct the geometry for this radially symmetrical fluid space is to generate a "slice" of the geometry and sweep it around an axis to create a cylinder.

To create the slice, open the geometry tab from the toolbar and select "create point." In the menu this opens, select "explicit coordinates" as shown in Figure 5. This allows a point to be created from Cartesian coordinates. In this three axis system, the two-dimensional slice will be created on the X-Y plane and rotated through the third dimension. As such, all Z-values will be 0 for this part of the procedure.
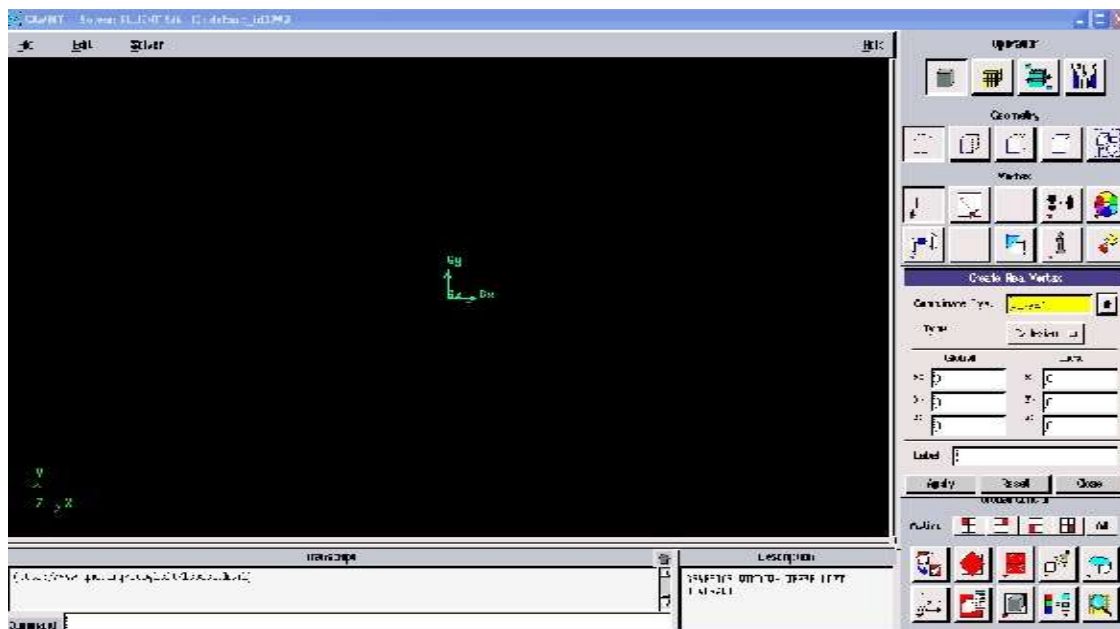

Fig. 18.

4.3.1 1ST GEOMETRY (INNER DIAMETER 2M)

To construct the concentrator, disk coordinate (2, 2, 0) , (2, 3, 0) , (2, 8, 0) , (1, 8, 0) , (1, 3, 0) and(2, 0, 0) , (2 ,-1, 0) , (2, -6, 0) , (1, -6, 0) , (1, -1,) by entering the coordinates in the spaces and joining line and curve as shown below.

And tunnel coordinate (90, 90, 0), (-90. 90. 0), (-90, -90, 0) and (90, -90, 0)

Fig. 19.

This will create a rim of the concentrator with a 2.0 m radius to be located at the origin

Now, using the point input methods, create the geometry of the concentrator and the tunnel. In models created for this thesis, this was done by plotting a set of 10-15 points for the profile of the concentrator. The line generation tool "from points" is robust in this program and will provide a smooth contour by selecting multiple points in succession before confirming the line. Multiple lines can be used to create sharp angles, such as at the rim of the concentrator to reduce turbulence.

After joining line all vertices make edge by joining points, make faces one is of tunnel and other is of concentrator body. Now we have 3 faces.

Face1 of coordinate (90, 90, 0), (-90, 90, 0), (-90, -90, 0) and (90, -90, 0)

Face2 of coordinate (2, 2, 0), (2, 3, 0), (2, 8, 0), (1, 8, 0), (1, 3, 0) and

Face3 of coordinate (2, 0, 0), (2,-1, 0), (2, -6, 0), (1, -6, 0), (1, -1, 0)

Now subtract face2 &3 from face1

After subtraction mesh faces by using menu MESH
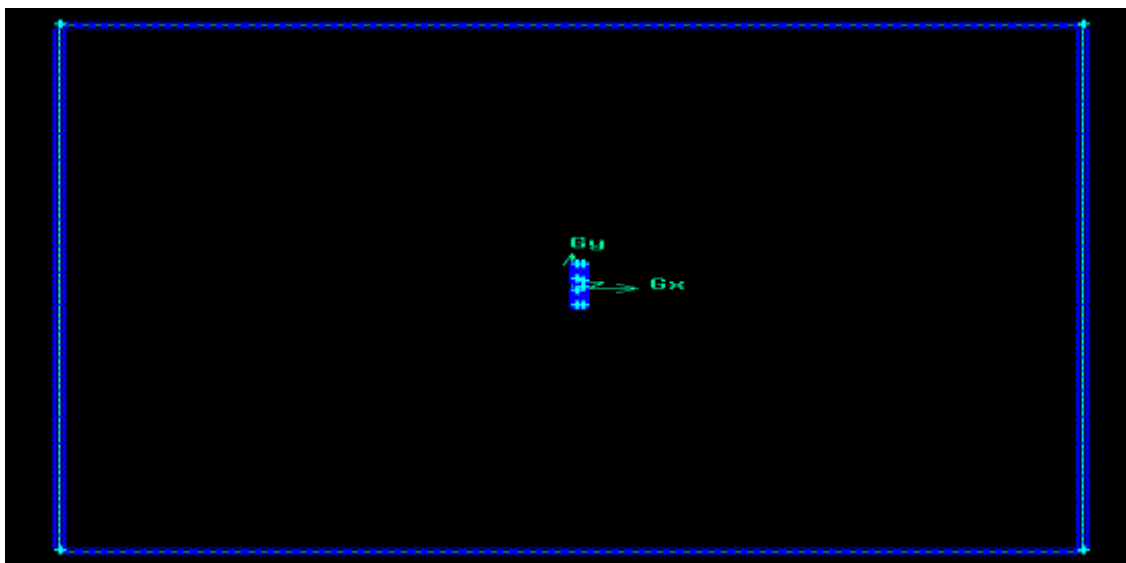
Fig. 20. Part creation

After these two parts have been created (for a total of three), the model is ready to have a mesh applied to it. Select the "Mesh" menu, located next to the geometry tab. For a well-sculpted mesh for these models set the number of nodes to 40 (see Figure 20).

Using the "advanced bunching" drop-down menu (selecting uniform) to ensure a good mesh size. For a model with a large cone, such as this example, a 40 node curve will suffice.

After the number of nodes per curve is established, the mesh may be generated. To generate the mesh, select the "Compute Mesh" icon, located at the right end of the "Mesh" tab. Select "compute" (located in the lower left corner) in the new menu without changing any other settings. If a dialog states that a mesh already exists, choose to replace that mesh with the new one by selecting "replace."

The mesh is now ready to be exported to fluent. To do this, first save the project. Next, select the "Output" tab from the top menu. Select the red tool box icon, whose tooltip reads "Select Solver." In the dropdown menu that results, select "Fluent V6." Now select the "Write Output" icon. Save the project if prompted, and open the corresponding .cas file for output. Name the file appropriately (in Figure 21, "EXAMPLE") and select "done." The mesh is now complete and ready to be loaded into Fluent.

The output file is found at the location written in the "Output file" prompt (shown in Figure21).
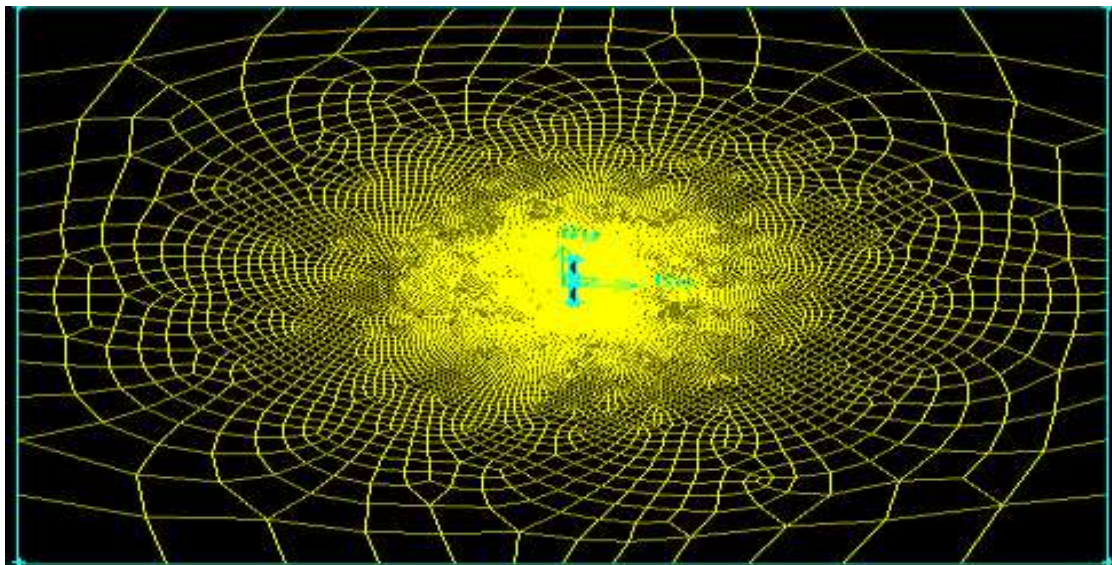

Fig. 21. MESH FILE 1

EDGE	INLET COUNT	INLET SIZE	RATIO
INLET/OUTLET	15	12	0.8
TOP/BOTTOM	12	15	0.8
BODY BACK	16	0.61	1
BODY CURVE	15	0.133	1
BODY FRONT	12	1	1
BODY TOP	8	1	1

4.3.2 2ND GEOMETRY (INNER DIAMETER 4M)

Similarly, we follow the steps as done to make mesh file 1

So, to construct the concentrator , disk coordinate (2, 2, 0) , (2, 3, 0) , (2, 10, 0) , (1, 10, 0) , (1, 3, 0) and(2, 0, 0) , (2 ,-1, 0) , (2, -8, 0) , (1, -8, 0) , (1, -1, 0) by entering the coordinates in the spaces and joining line and curve as shown below.

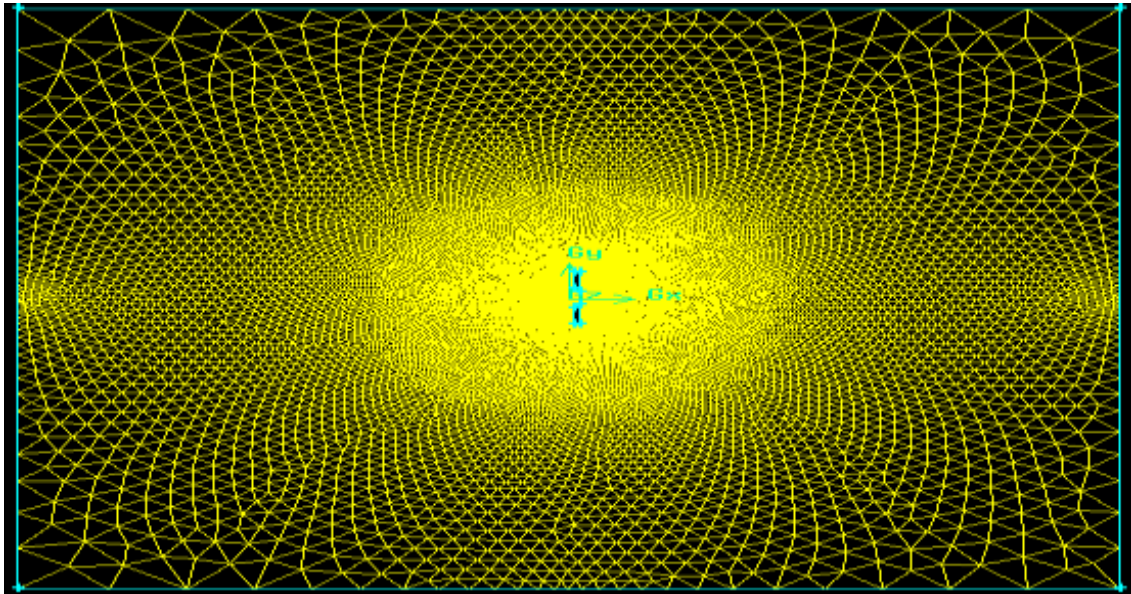And tunnel coordinate (90, 90, 0), (-90. 90. 0), (-90, -90, 0) and (90, -90, 0)

Fig. 22. MESH FILE 2

EDGE	INLET COUNT	INLET SIZE	RATIO
INLET/OUTLET	40	5.0	0.866
TOP/BOTTOM	26	6.923	0.855
BODY BACK	20	0.3	1
BODY CURVE	8	0.25	1
BODY FRONT	10	0.5	1
BODY TOP	5	0.2	1

4.3.3 3RD GEOMETRY (INNER DIAMETER 6M)

Similarly, we follow the steps as done to make mesh file 1

So, to construct the concentrator , disk coordinate (2, 2, 0) , (2, 3, 0) , (2, 12, 0) , (1, 12, 0) , (1, 3, 0) and(2, 0, 0) , (2 ,-1, 0) , (2, -10, 0) , (1, -10, 0) , (1, -1,) by 2ntering the coordinates in the spaces and joining line and curve as shown below.

And tunnel coordinate (90, 90, 0) , (-90. 90. 0), (-90, -90, 0) and (90, -90, 0)
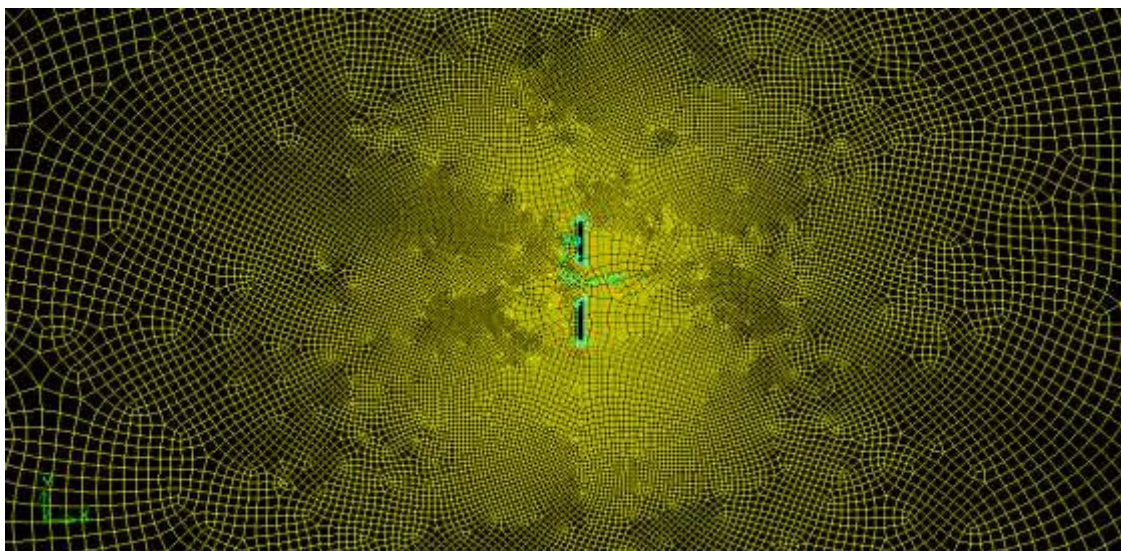
Fig. 23. MESH FILE 3

EDGE	INLET COUNT	INLET SIZE	RATIO
INLET/OUTLET	40	12	0.86
TOP/BOTTOM	20	24	0.855
BODY BACK	20	0.35	1
BODY CURVE	8	1	1
BODY FRONT	10	0.6	1
BODY TOP	6	0.16	1

4.4 Problem Solving in Fluent

To format the file in Fluent, begin by opening Fluent in 2D mode. Select "File" from the top toolbar, and select "Read"=>"Case,.,." Open the output file. The model will be properly scaled already, as Fluent's default unit of length is the meter. Now, become familiar with the Problem Setup menu on the left side of the screen. This is used to set the boundary conditions of the problem**.**
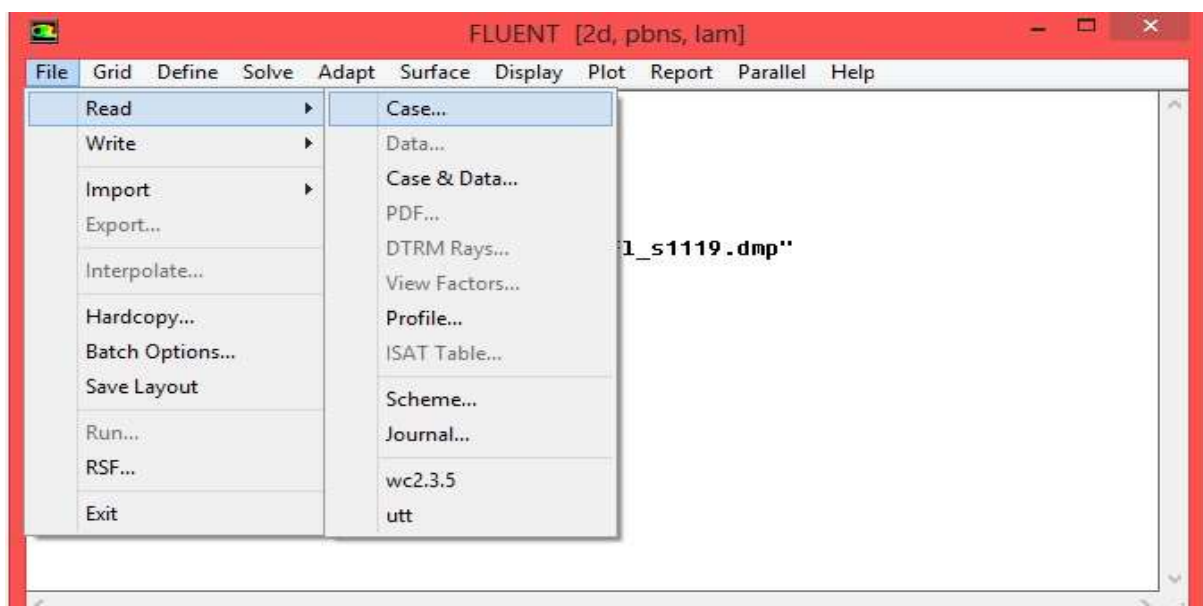
Fig. 24: File Menu
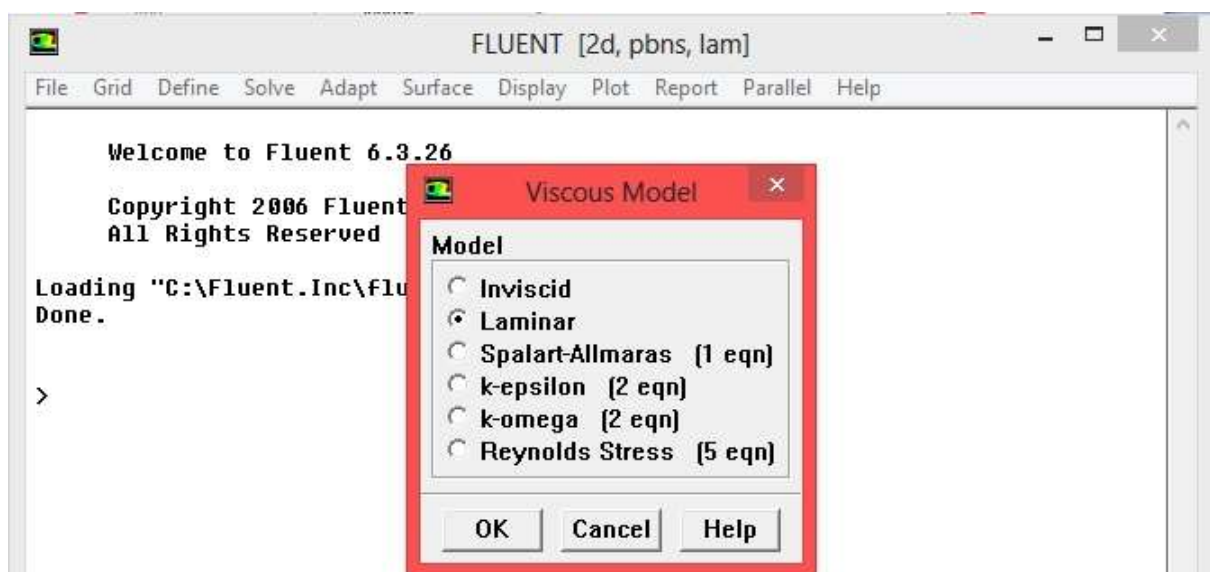
Fig. 25: Viscous Model

Page | 71

The first thing to be modified is the "Models" selection. In this selection, the "Viscous" model should be the default (laminar) . This is as shown in Figure 25.

Select "Define material" after this has been completed and ensures that Air is the fluid in the fluid-space of the model. This is done by selecting "Fluent Fluid Material…" ensuring "air" is listed as the fluid in the drop-down menu titled "Material Name" (See Figure 26).
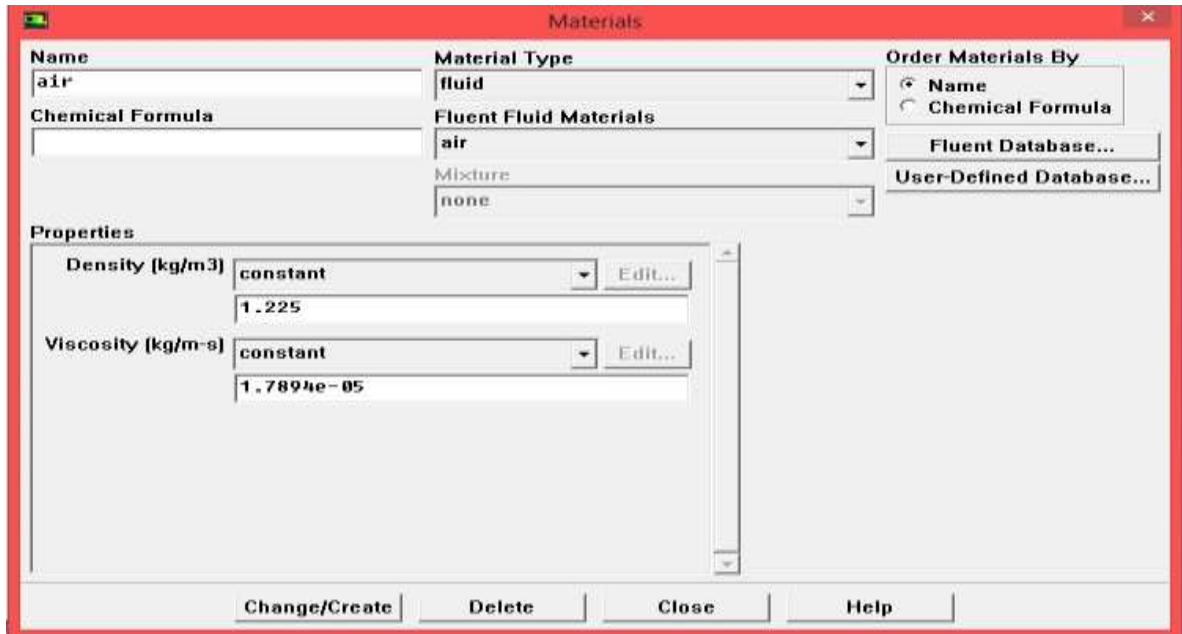

Fig. 26: Material Name

Next, choose "Boundary Conditions." Fluent will display the parts of the model that were established in GAMBIT, the internal mesh, the wall mesh describing the wall and the concentrator, the VEL_IN, and the VEL_OUT regions. The wall mesh will already be defined as a "Wall" boundary, and the internal mesh will be defined as "Interior" . The remaining two zones should be defined as such: VEL_IN (or similar name depending on the nomenclature used when creating the mesh) should be a "mass flow inlet." This choice can be selected by highlighting VEL_IN and choosing this from the "Type" dropdown menu. This will bring up another menu, in which one may modify the mass flow rate. The mass flow rate at experimental conditions is 223.15 kg/s as shown in Figure 27.
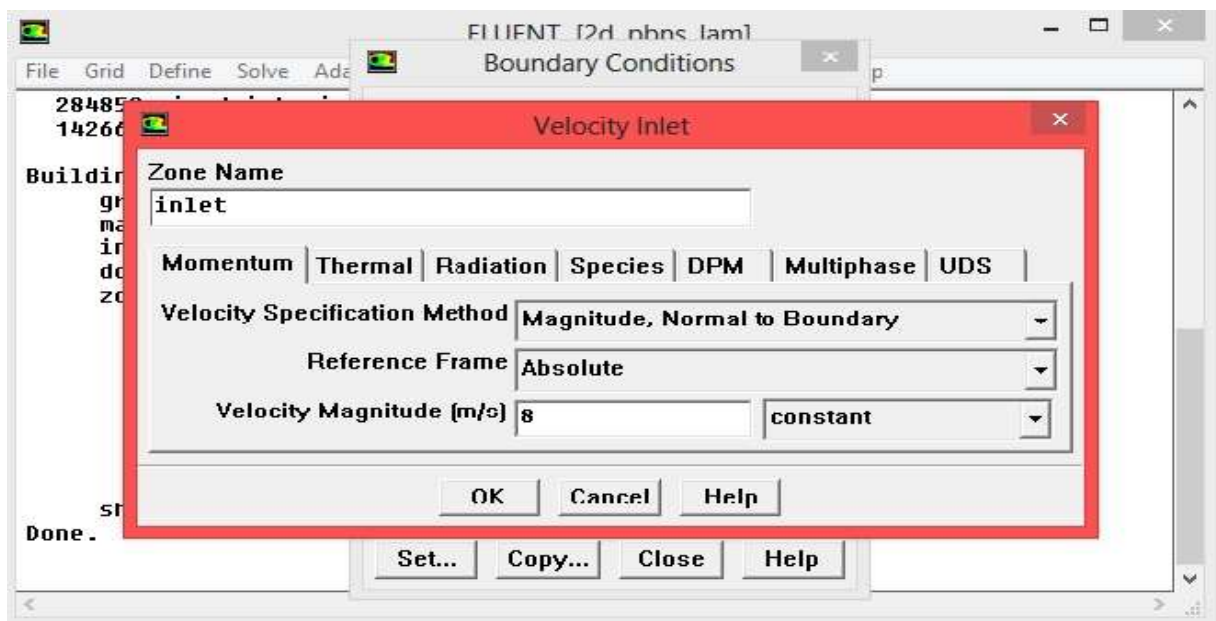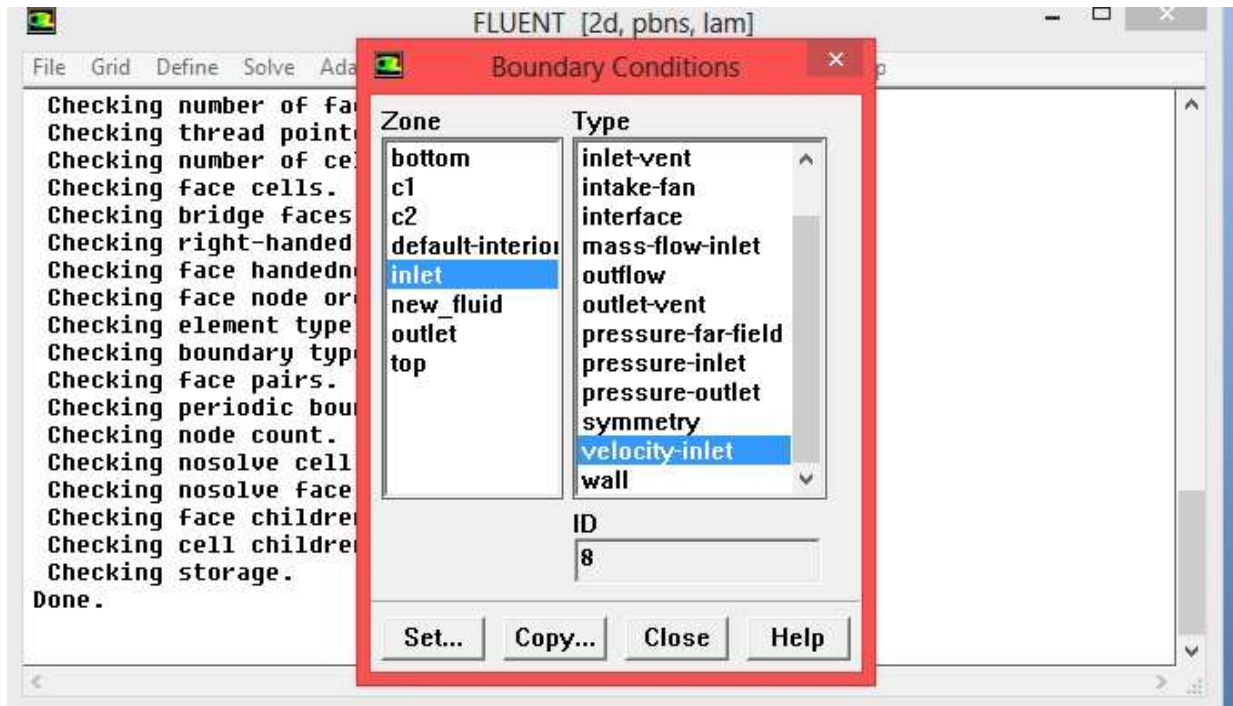

Fig. 27: Velocity inlet

Fig. 28: Boundary Conditions

Now highlight VEL_OUT, and select the type "pressure-outlet. This will bring up another window. Nothing should be changed here; simply select OK to close the window. This concludes the problem setup for this model.

Now begin to define the solution methods, listed in the "Solution Control" menu. Here, select "pressure-Velocity coupling" from the "Scheme" dropdown menu, and select the options 'SIMPLE' shown in Figure 29.

Now, select "Solution Controls." Here, the Under-Relaxation factors may be adjusted. These factors are used to determine how quickly the calculations may converge; too high and the calculation will often diverge, while if too low, a solution will never be reached. A good starting point for these values is as shown in Figure 29. These may be altered as needed. The other factors should not be changed.
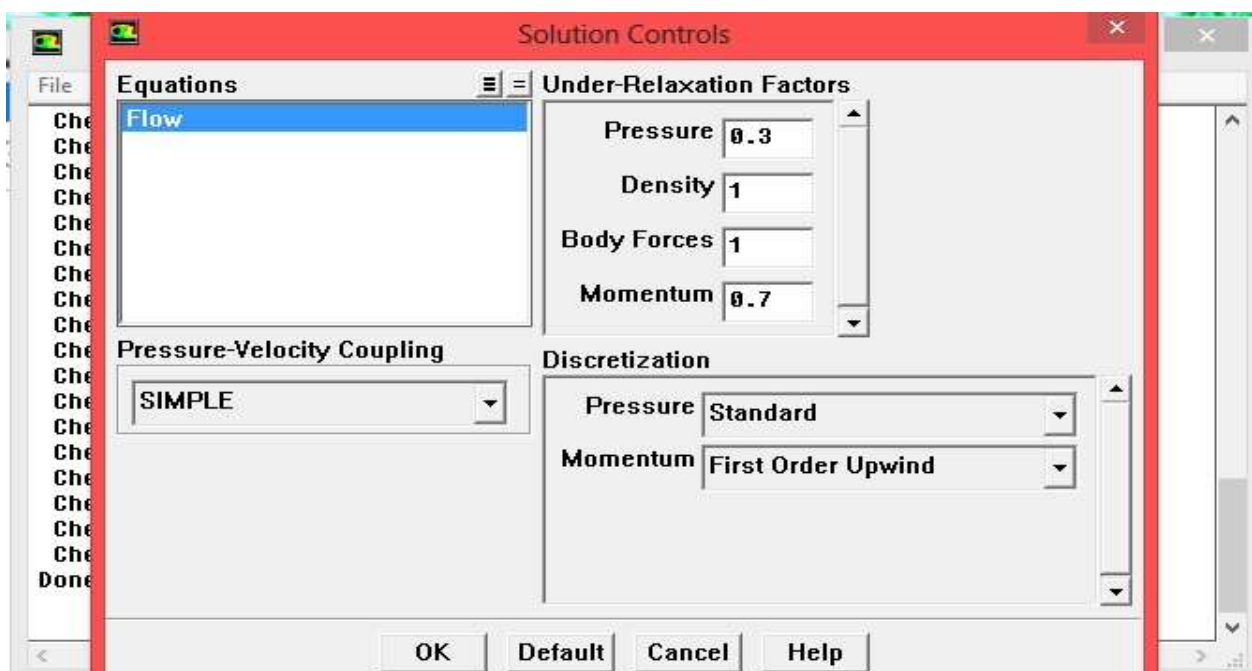

Fig. 29. Solution Controls

SIMPLE Algorithm

In present analysis SIMPLE (Semi-Implicit Method For Pressure Linked Equations) algorithm is used because It is very user friendly numerical procedure to solve the Navier-Stokes equations. The main objective behind using this algorithm is it solves the pressure and velocity iteratively for example if a steady-state problem is being solved iteratively, it is not necessary to fully resolve the linear pressure-velocity coupling, with the help of simple algorithm it can be easily solved .

In the SIMPLE algorithm:-

- An approximation of the velocity field is obtained by solving the momentum equation. The pressure gradient term is calculated using the pressure distribution from the previous iteration or an initial guess.

- The pressure equation is formulated and solved in order to obtain the new pressure distribution.

- Velocities are corrected and a new set of conservative fluxes is calculated.

Fig. 30

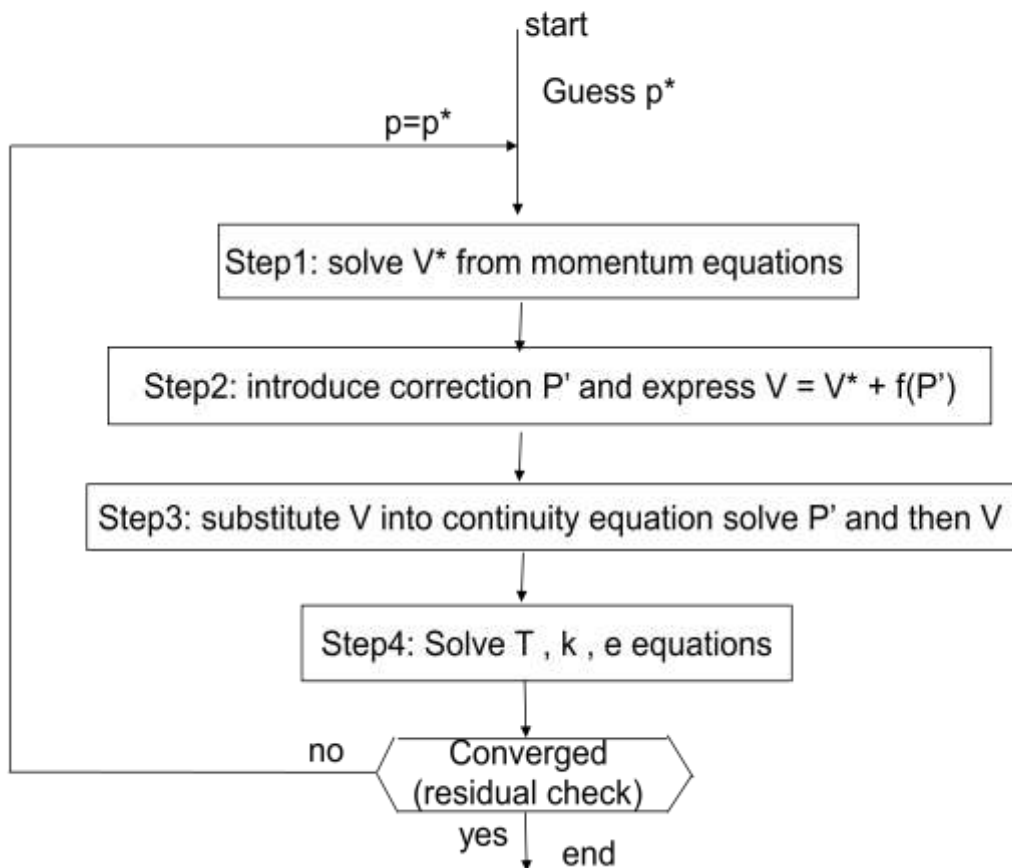Next, Select the "Monitors" option next and highlight "Residuals Monitors – Print, Plot." Press the "Edit…" button and increase the "Absolute Criteria" for all values to 1e-05 as in Figure 1. Press "OK" to confirm the alterations. This will allow calculations to continue until there is no variance in iterations greater than 0.00001 units.
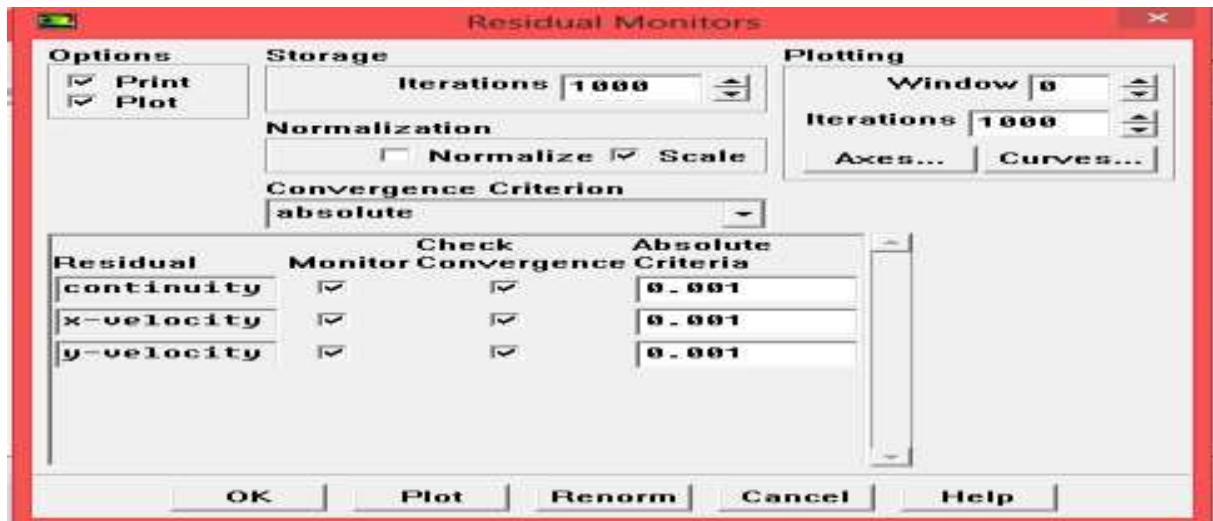
Select the "Monitors" option next and highlight "Residuals Monitors – Print, Plot." Press the "Edit…" button and increase the "Absolute Criteria" for all values to 1e-05 as in Figure 31. Press "OK" to confirm the alterations. This will allow calculations to continue until there is no variance in iterations greater than 0.00001 units.

Fig. 31. Monitors Residual

Select the "Solution Initialization" below "Monitors" now, and press the "Initialize" button to prepare the model for use (See Figure 32). Lastly, select "Iterate.,.,.,." input the number of iterations desired (generally 1000 or more) and press calculate. After beginning calculations, wait until the calculation is completed by Fluent (signified by a window stating that convergence has occurred).
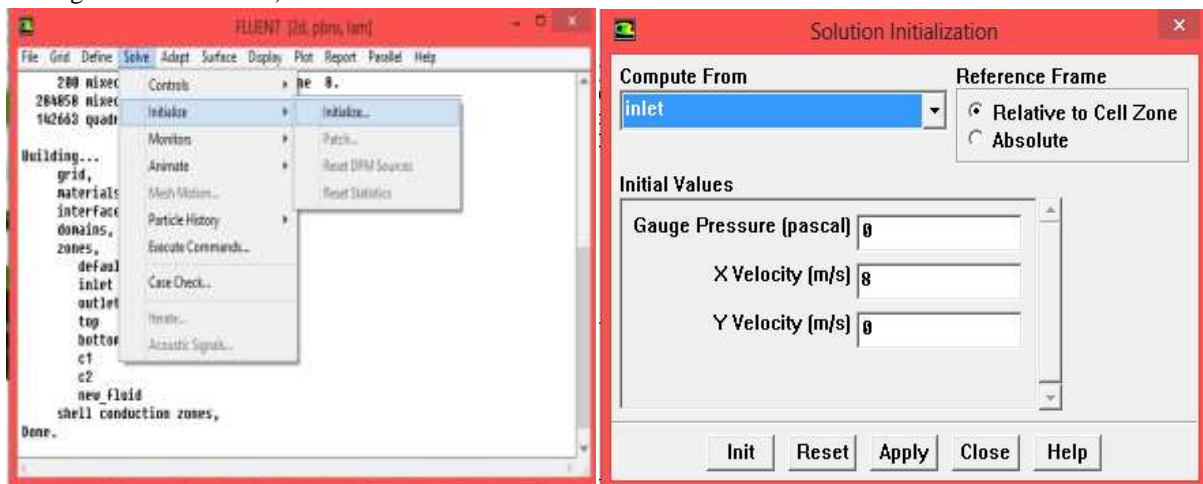

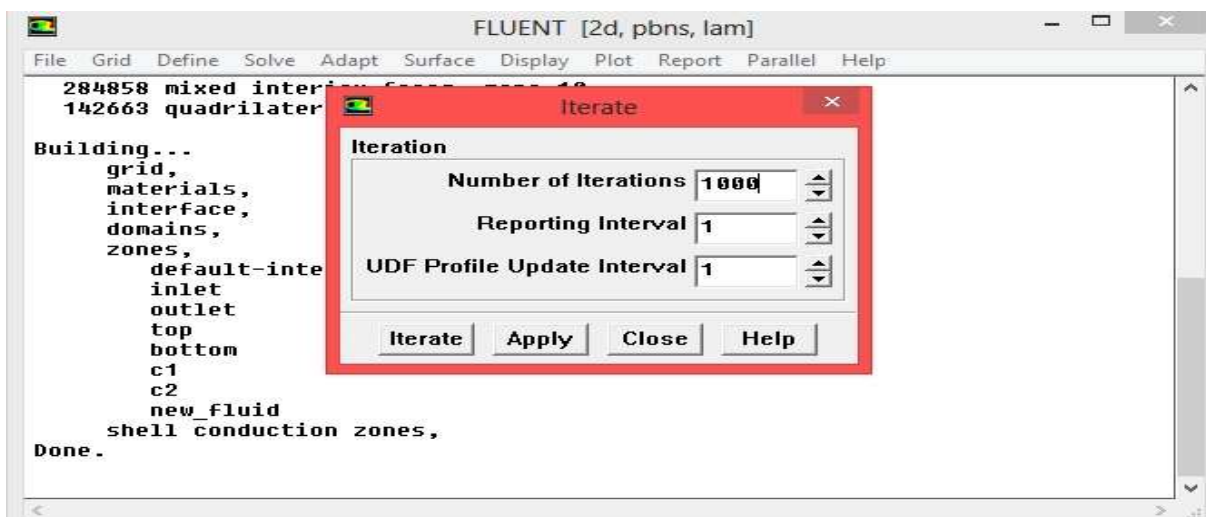**Fig. 32. Initialization and Calculation**

Fig. 33. Iteration

4.5 Viewing Results

To view the velocity and turbulence profile of the model, select 'Counter' under "Display," highlight "Surfaces" box, and select the desired property from the "Counter of…" menu. While designing the concentrator, this procedure for model creation and data collection proved effective in all cases.
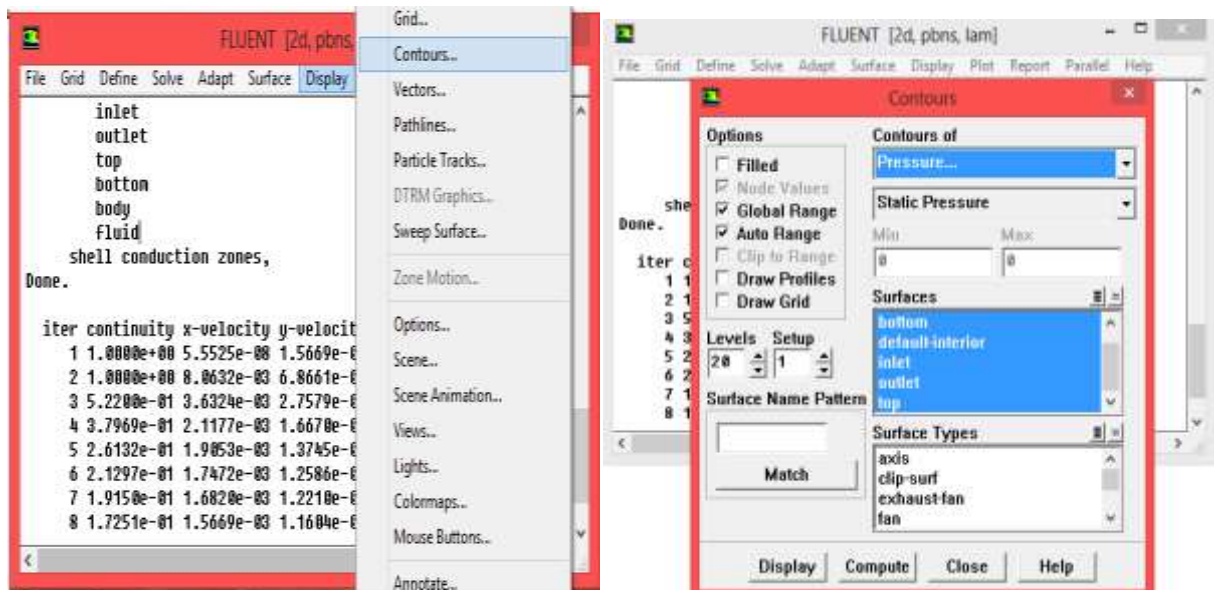

Fig. 34. Viewing Results

V.   RESULT AND DISCUSSION

The results concluded out by analytical method through several circular disk shaped concentrator given below:

INNER DIAMETER OF CONCENTRATOR (m)	OUTLET VELOCITY (m/s)
2	56
4	32.32
6	24.24

Here, we assume several conditions i.e. the flow is steady state, incompressible and consider the value of ρ and μ at room temperature. The inlet velocity v is 8m/s for all three selected concentrator.

Next, numerical analysis using CFD conducted on the concentrator outlet velocity, pressure, Reynolds number affected by the different geometry of concentrators under same discritizing flow.
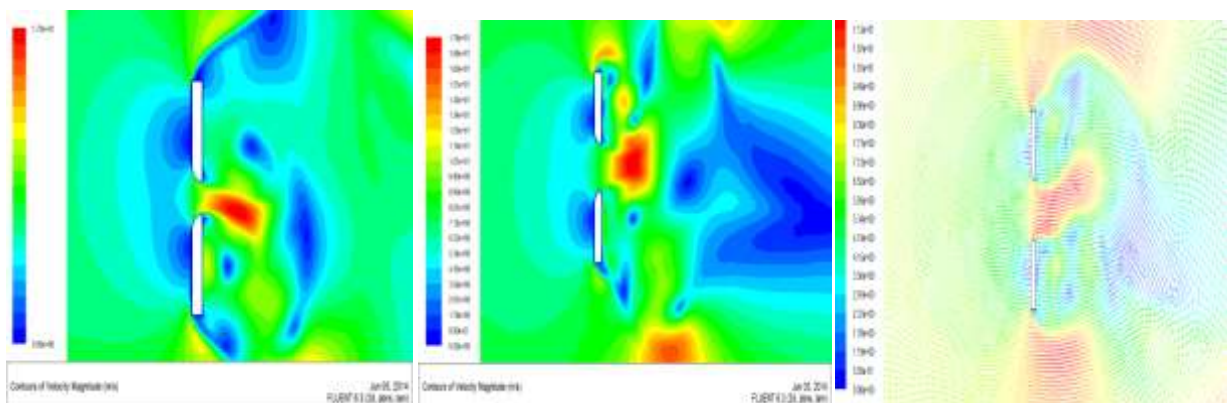

Fig. 35. Velocity Contour

a. (d=2m)   b. (d=4m)   c. (d=6m)

The above figure35. shows the velocity magnitude results concluded out through different inner radius of concentrator as mention in fig. for same inlet velocity we get v_1 =17.2m/s, v_2 = 17.8m/s, v_3 =13m/s respectively.

The figure shows the pressure magnitude results concluded out through different inner radius of concentrator as mention in fig. for same inlet pressure we get P_1=5atm, P_2=5atm, P_3=4.2atm respectively

Fig. 36. Pressure Contour

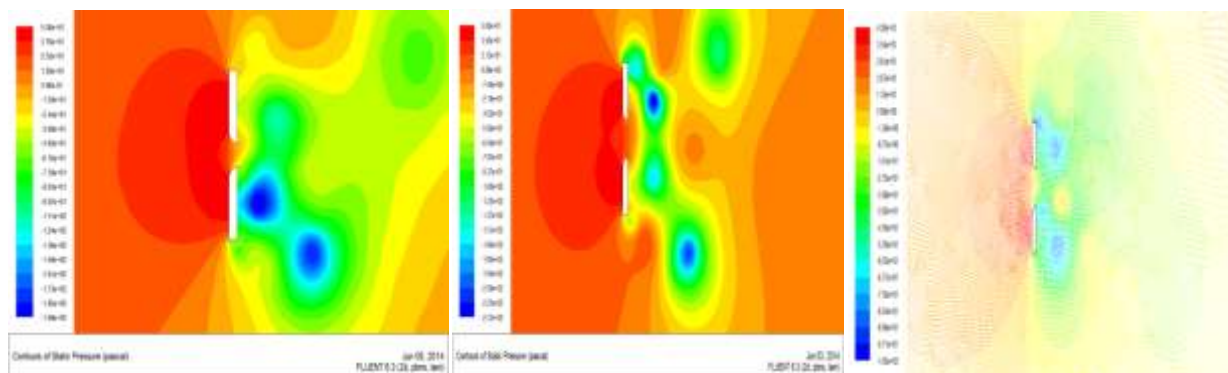a. (d=2m)   b. (d=4m)   c. (d=6m)
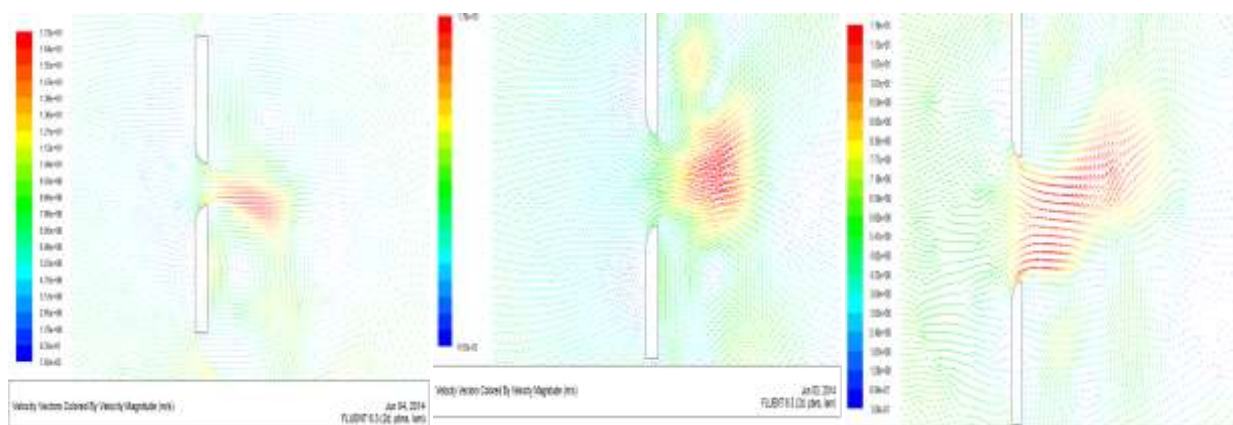

Fig. 37. Velocity Vector

a. (d=2m)   b. (d=4m)   c. (d=6m)

The above figure shows the velocity vector results through different inner radius of concentrator as mention in fig. with this we concluded out in which one the flow is uniform and unidirectional perfectly up to certain distance and time.

Now finally the different theoretical velocity, CFD analysis velocities and the Reynolds number concluded out through different concentrator area are given below:

Inner radius Of Concentrator (m)	Theoretical Velocities (m/s)	CFD analysis Velocities (m/s)	Reynolds No.
2	56	17.2	5.648008×10^5
4	32.32	17.8	6.5194×10^5
6	24.24	13	7.334×10^5

The data in table shows how changes occur in velocities and Reynolds numbers when area of concentrator changes.

VI. CONCLUSION

- A properly designed Circular Disk concentrator can be used to increase the effectiveness of a wind.

- A Disk having Dia. 4m is most effective at reduced flow separation and increasing velocity, Improving wind speed to 17.8m/s more than other analyzed cases.

- Designs of circular Disk Dia. 2m is not much effective due to high turbulence and flow separation in systems composed of low density fluids such as air.

- Pressure relief is possible by design optimization and are effective at both reducing turbulence and producing a flow rectified with the circular Disk concentrator geometry, increasing maximum velocity by 44%.

- The final design, Disk with Dia. 4m transfers 76% of the momentum present at the entrance to the throat, with an overall increase in velocity of 222.5%, from 8 m/s to 17.8 m/s.

- Experimental data from the prototype performed within 8% of expectations, For validating the present CFD model.

RECOMMENDATIONS

- Further optimization could be streamlined through the use of Linux coding to generate models of a certain type and perform "hands-off" optimizations of fine parameters such as slight width, concentrator diameter or concentrator profile.

- Investigate the effect of different types of turbine blades on power generation and effects of back-pressure.

- Re-optimize Disk Concentrator Design and location with respect to different blade designs.

- Re-optimize Disk curvature and diameter with respect to the shortened inlet size and make effective use of low density wind.

- Aerodynamically better geometries can be analyzed in future to reduce the flow separation and loses incorporated in present design.

- To validate the present model an experimental setup of model dimension can be built and analyzed for different flow conditions.

REFERENCES

[1] AGARDOGRAPH No. 243, Fluid Dynamic Aspects of Wind Energy Conversion by O. de. Vries, National Aerospace Laboratory NLR, Anthony Fokkerweg 2, 1059 CM Amsterdam, The Netherlands

[2] ALLNOCH, N., 1992: Windkraftnutzung im nordwestdeutschen Binnenland: Ein System zur Standortbewertung f¨ur Windkraftanlagen. – Geographische Kommission f¨ur Westfalen, M¨unster, ARDEY-Verlag, 160 pp (cited from H¨A NSCH, 1997).

[3] ANSYS, Inc. 2009. FLUENT 12.0 Theory Guide. ANSYS.

[4] CFD modeling, 4858 wind accelerator by Michael D. Lucas B. S., University of Louisville, 2010.

[5] Chung, T. J. 2002. Computational Fluid Dynamics. Cambridge, UK: Cambridge University Press

[6] Davis, Edward L. 2010. US Patent 2010/0111689.

[7] Ferziger et al, J. H. 2002. Computational Methods for Fluid Dynamics Third Edition. New York: Springer-Verlag.

[8] FRANKLIN, J. L., C. A Avila, J. L. Beven, M. B. Lawrence, R. J. Pasch, and S. R. Stewart, 2001: Atlantic hurricane season of 2000. Mon. Wea. Rev., 129, 3037 - 3056.

[9] HYDRAULICS CONCEPT by Prof. B.S.Thandaveswara, IIT Madars & Assit. Prof. Ram Niwas Bishnoi, NIMS University, Jaipur

[10] Russ. David. 2011. "CFD Modeling of Entrance and Exit Geometries of Wind Speed Accelerators." University of Louisville: Speed School of Engineering.

[11] SUZLON POWERING A GREENER TOMORROW, annual report 2012-2013, www.suzlon.com

[12] WIND ENERGY IN THE BUILT ENVIRONMENT,CONCENTRATOR EFFECTS OF BUILDINGS, Published by: Multi-Science, 5 Wates Way, Brentwood, Essex, CM15 9TB, United Kingdom, ISBN 0906522 35 8

[13] WORLD WIND ENERGY ASSOCIATION, Retrieval 31 October, 2012.